Journal of Computational Physics 229 (2010) 7874–7892

Contents lists available at ScienceDirect

Journal of Computational Physics

journal homepage: www.elsevier.com/locate/jcp

Efficient numerical methods for computing ground states and dynamics of dipolar Bose–Einstein condensates

Weizhu Bao [a,b,*], Yongyong Cai [a], Hanquan Wang [a,c]

[a] Department of Mathematics, National University of Singapore, 117543, Singapore
[b] Center for Computational Science and Engineering, National University of Singapore, 117543, Singapore
[c] School of Statistics and Mathematics, Yunnan University of Finance and Economics, PR China

ARTICLE INFO

Article history:
Received 14 January 2010
Accepted 1 July 2010
Available online 8 July 2010

Keywords:
Dipolar Bose–Einstein condensate
Gross–Pitaevskii equation
Dipolar interaction potential
Gross–Pitaevskii–Poisson type system
Ground state
Backward Euler sine pseudospectral method
Time-splitting sine pseudospectral method

ABSTRACT

New efficient and accurate numerical methods are proposed to compute ground states and dynamics of dipolar Bose–Einstein condensates (BECs) described by a three-dimensional (3D) Gross–Pitaevskii equation (GPE) with a dipolar interaction potential. Due to the high singularity in the dipolar interaction potential, it brings significant difficulties in mathematical analysis and numerical simulations of dipolar BECs. In this paper, by decoupling the two-body dipolar interaction potential into short-range (or local) and long-range interactions (or repulsive and attractive interactions), the GPE for dipolar BECs is reformulated as a Gross–Pitaevskii–Poisson type system. Based on this new mathematical formulation, we prove rigorously existence and uniqueness as well as nonexistence of the ground states, and discuss the existence of global weak solution and finite time blow-up of the dynamics in different parameter regimes of dipolar BECs. In addition, a backward Euler sine pseudospectral method is presented for computing the ground states and a time-splitting sine pseudospectral method is proposed for computing the dynamics of dipolar BECs. Due to the adoption of new mathematical formulation, our new numerical methods avoid evaluating integrals with high singularity and thus they are more efficient and accurate than those numerical methods currently used in the literatures for solving the problem. Extensive numerical examples in 3D are reported to demonstrate the efficiency and accuracy of our new numerical methods for computing the ground states and dynamics of dipolar BECs.

1. Introduction

Since 1995, the Bose–Einstein condensation (BEC) of ultracold atomic and molecular gases has attracted considerable interests both theoretically and experimentally. These trapped quantum gases are very dilute and most of their properties are governed by the interactions between particles in the condensate [31]. In the last several years, there has been a quest for realizing a novel kind of quantum gases with the dipolar interaction, acting between particles having a permanent magnetic or electric dipole moment. A major breakthrough has been very recently performed at Stuttgart University, where a BEC of ^{52}Cr atoms has been realized in experiment and it allows the experimental investigations of the unique properties of dipolar quantum gases [22]. In addition, recent experimental developments on cooling and trapping of molecules [17], on photoassociation [43], and on Feshbach resonances of binary mixtures open much more exciting perspectives towards a degenerate quantum gas of polar molecules [35]. These success of experiments have spurred great excitement in the atomic physics

* Corresponding author at: Department of Mathematics, National University of Singapore, 117543, Singapore.
E-mail addresses: bao@math.nus.edu.sg (W. Bao), caiyongyong@nus.edu.sg (Y. Cai), hanquan.wang@gmail.com (H. Wang).

0021-9991/$ - see front matter © 2010 Elsevier Inc. All rights reserved.
doi:10.1016/j.jcp.2010.07.001

community and renewed interests in studying the ground states [36,48,20,21,23,34] and dynamics [25,30,32,50] of dipolar BECs.

At temperature T much smaller than the critical temperature T_c, a dipolar BEC is well described by the macroscopic wave function $\psi = \psi(\mathbf{x}, t)$ whose evolution is governed by the three-dimensional (3D) Gross–Pitaevskii equation (GPE) [48,36]

$$i\hbar\partial_t\psi(\mathbf{x},t) = \left[-\frac{\hbar^2}{2m}\nabla^2 + V(\mathbf{x}) + U_0|\psi|^2 + \left(V_{\rm dip} * |\psi|^2\right)\right]\psi, \quad \mathbf{x}\in\mathbb{R}^3,\ t>0, \tag{1.1}$$

where t is time, $\mathbf{x} = (x,y,z)^T \in \mathbb{R}^3$ is the Cartesian coordinates, $\hbar$ is the Planck constant, m is the mass of a dipolar particle and $V(\mathbf{x})$ is an external trapping potential. When a harmonic trap potential is considered, $V(\mathbf{x}) = \frac{m}{2}(\omega_x^2x^2 + \omega_y^2y^2 + \omega_z^2z^2)$ with ω_x, ω_y and ω_z being the trap frequencies in x-, y- and z-directions, respectively. $U_0 = \frac{4\pi\hbar^2 a_s}{m}$ describes local (or short-range) interaction between dipoles in the condensate with a_s the s-wave scattering length (positive for repulsive interaction and negative for attractive interaction). The long-range dipolar interaction potential between two dipoles is given by

$$V_{\rm dip}(\mathbf{x}) = \frac{\mu_0\mu_{\rm dip}^2}{4\pi}\frac{1-3(\mathbf{x}\cdot\mathbf{n})^2/|\mathbf{x}|^2}{|\mathbf{x}|^3} = \frac{\mu_0\mu_{\rm dip}^2}{4\pi}\frac{1-3\cos^2(\theta)}{|\mathbf{x}|^3}, \qquad \mathbf{x}\in\mathbb{R}^3, \tag{1.2}$$

where μ_0 is the vacuum magnetic permeability, $\mu_{\rm dip}$ is permanent magnetic dipole moment (e.g. $\mu_{\rm dip} = 6\mu_B$ for $^{52}C_r$ with μ_B being the Bohr magneton), $\mathbf{n} = (n_1,n_2,n_3)^T \in \mathbb{R}^3$ is the dipole axis (or dipole moment) which is a given unit vector, i.e. $|\mathbf{n}| = \sqrt{n_1^2+n_2^2+n_3^2} = 1$, and θ is the angle between the dipole axis $\mathbf{n}$ and the vector $\mathbf{x}$. The wave function is normalized according to

$$\|\psi\|^2 := \int_{\mathbb{R}^3} |\psi(\mathbf{x},t)|^2\, d\mathbf{x} = N, \tag{1.3}$$

where N is the total number of dipolar particles in the dipolar BEC.

By introducing the dimensionless variables, $t \to \frac{t}{\omega_0}$ with $\omega_0 = \min\{\omega_x,\omega_y,\omega_z\}$, $\mathbf{x} \to a_0\mathbf{x}$ with $a_0 = \sqrt{\frac{\hbar}{m\omega_0}}$, $\psi \to \frac{\sqrt{N}\psi}{a_0^{3/2}}$, we obtain the dimensionless GPE in 3D from (1.1) as [48,49,31,5]:

$$i\partial_t\psi(\mathbf{x},t) = \left[-\frac{1}{2}\nabla^2 + V(\mathbf{x}) + \beta|\psi|^2 + \lambda\left(U_{\rm dip} * |\psi|^2\right)\right]\psi, \qquad \mathbf{x}\in\mathbb{R}^3,\ t>0, \tag{1.4}$$

where $\beta = \frac{NU_0}{\hbar\omega_0 a_0^3} = \frac{4\pi a_s N}{a_0}$, $\lambda = \frac{mN\mu_0\mu_{\rm dip}^2}{3\hbar^2 a_0}$, $V(\mathbf{x}) = \frac{1}{2}(\gamma_x^2x^2 + \gamma_y^2y^2 + \gamma_z^2z^2)$ is the dimensionless harmonic trapping potential with $\gamma_x = \frac{\omega_x}{\omega_0}$, $\gamma_y = \frac{\omega_y}{\omega_0}$ and $\gamma_z = \frac{\omega_z}{\omega_0}$, and the dimensionless long-range dipolar interaction potential $U_{\rm dip}(\mathbf{x})$ is given as

$$U_{\rm dip}(\mathbf{x}) = \frac{3}{4\pi}\frac{1-3(\mathbf{x}\cdot\mathbf{n})^2/|\mathbf{x}|^2}{|\mathbf{x}|^3} = \frac{3}{4\pi}\frac{1-3\cos^2(\theta)}{|\mathbf{x}|^3}, \qquad \mathbf{x}\in\mathbb{R}^3. \tag{1.5}$$

From now on, we will treat β and λ as two dimensionless real parameters. We understand that it may not physically meaningful when $\lambda < 0$ for modeling dipolar BEC. However, it is an interesting problem to consider the case when $\lambda < 0$ at least in mathematics and it may make sense for modeling other physical system. In fact, the above nondimensionlization is obtained by adopting a unit system where the units for length, time and energy are given by a_0, $1/\omega_0$ and $\hbar\omega_0$, respectively. Two important invariants of (1.4) are the *mass* (or normalization) of the wave function

$$N(\psi(\cdot,t)) := \|\psi(\cdot,t)\|^2 = \int_{\mathbb{R}^3} |\psi(\mathbf{x},t)|^2\, d\mathbf{x} \equiv \int_{\mathbb{R}^3} |\psi(\mathbf{x},0)|^2\, d\mathbf{x} = 1, \qquad t \geqslant 0, \tag{1.6}$$

and the *energy* per particle

$$E(\psi(\cdot,t)) := \int_{\mathbb{R}^3}\left[\frac{1}{2}|\nabla\psi|^2 + V(\mathbf{x})|\psi|^2 + \frac{\beta}{2}|\psi|^4 + \frac{\lambda}{2}\left(U_{\rm dip} * |\psi|^2\right)|\psi|^2\right]d\mathbf{x} \equiv E(\psi(\cdot,0)), \qquad t \geqslant 0. \tag{1.7}$$

To find the stationary states including ground and excited states of a dipolar BEC, we take the ansatz

$$\psi(\mathbf{x},t) = e^{-i\mu t}\phi(\mathbf{x}), \qquad \mathbf{x}\in\mathbb{R}^3, \quad t \geqslant 0, \tag{1.8}$$

where $\mu \in \mathbb{R}$ is the chemical potential and $\phi := \phi(\mathbf{x})$ is a time-independent function. Plugging (1.8) into (1.4), we get the time-independent GPE (or a nonlinear eigenvalue problem)

$$\mu\phi(\mathbf{x}) = \left[-\frac{1}{2}\nabla^2 + V(\mathbf{x}) + \beta|\phi|^2 + \lambda\left(U_{\rm dip} * |\phi|^2\right)\right]\phi(\mathbf{x}), \qquad \mathbf{x}\in\mathbb{R}^3, \tag{1.9}$$

under the constraint

$$\|\phi\|^2 := \int_{\mathbb{R}^3} |\phi(\mathbf{x})|^2\, d\mathbf{x} = 1. \tag{1.10}$$

The ground state of a dipolar BEC is usually defined as the minimizer of the following nonconvex minimization problem:

Find $\phi_g \in S$ and $\mu^g \in \mathbb{R}$ such that

$$E^g := E(\phi_g) = \min_{\phi \in S} E(\phi), \qquad \mu^g := \mu(\phi_g), \tag{1.11}$$

where the nonconvex set S is defined as

$$S := \left\{ \phi \,|\, \|\phi\|^2 = 1, E(\phi) < \infty \right\} \tag{1.12}$$

and the chemical potential (or eigenvalue of (1.9)) is defined as

$$\mu(\phi) := \int_{\mathbb{R}^3} \left[\frac{1}{2} |\nabla \phi|^2 + V(\mathbf{x}) |\phi|^2 + \beta |\phi|^4 + \lambda \left(U_{\rm dip} * |\phi|^2 \right) |\phi|^2 \right] d\mathbf{x} \equiv E(\phi) + \frac{1}{2} \int_{\mathbb{R}^3} \left[\beta |\phi|^4 + \lambda \left(U_{\rm dip} * |\phi|^2 \right) |\phi|^2 \right] d\mathbf{x}. \tag{1.13}$$

In fact, the nonlinear eigenvalue problem (1.9) under the constraint (1.10) can be viewed as the Euler–Lagrangian equation of the nonconvex minimization problem (1.11). Any eigenfunction of the nonlinear eigenvalue problem (1.9) under the constraint (1.10) whose energy is larger than that of the ground state is usually called as an excited state in the physics literatures.

The theoretical study of dipolar BECs including ground states and dynamics as well as quantized vortices has been carried out in recent years based on the GPE (1.1). For the study in physics, we refer to [16,18,24,33,1,19,24,27,28,44,45,47,49,52] and references therein. For the study in mathematics, existence and uniqueness as well as the possible blow-up of solutions were studied in [12], and existence of solitary waves was proven in [2]. In most of the numerical methods used in the literatures for theoretically and/or numerically studying the ground states and dynamics of dipolar BECs, the way to deal with the convolution in (1.4) is usually to use the Fourier transform [25,20,34,46,10,41,51]. However, due to the high singularity in the dipolar interaction potential (1.5), there are two drawbacks in these numerical methods: (i) the Fourier transforms of the dipolar interaction potential (1.5) and the density function $|\psi|^2$ are usually carried out in the continuous level on the whole space $\mathbb{R}^3$ (see (2.3) for details) and in the discrete level on a bounded computational domain Ω, respectively, and due to this mismatch, there is a locking phenomena in practical computation as observed in [34]; (ii) the second term in the Fourier transform of the dipolar interaction potential is $\frac{0}{0}$-type for 0-mode, i.e. when $\xi = 0$ (see (2.3) for details), and it is artificially omitted when $\xi = 0$ in practical computation [34,21,29,50,49,46,10] thus this may cause some numerical problems too. The main aim of this paper is to propose new numerical methods for computing ground states and dynamics of dipolar BECs which can avoid the above two drawbacks and thus they are more accurate than those currently used in the literatures. The key step is to decouple the dipolar interaction potential into a short-range and a long-range interaction (see (2.5) for details) and thus we can reformulate the GPE (1.4) into a Gross–Pitaevskii–Poisson type system. In addition, based on the new mathematical formulation, we can prove existence and uniqueness as well as nonexistence of the ground states and discuss mathematically the dynamical properties of dipolar BECs in different parameter regimes.

The paper is organized as follows. In Section 2, we reformulate the GPE for a dipolar BEC into a Gross–Pitaevskii–Poisson type system and study analytically the ground states and dynamics of dipolar BECs. In Section 3, a backward Euler sine pseudospectral method is proposed for computing ground states of dipolar BECs; and in Section 4, a time-splitting sine pseudospectral (TSSP) method is presented for computing the dynamics. Extensive numerical results are reported in Section 5 to demonstrate the efficiency and accuracy of our new numerical methods. Finally, some conclusions are drawn in Section 6. Throughout this paper, we adopt the standard Sobolev spaces and their corresponding norms.

2. Analytical results for ground states and dynamics

Let $r = |\mathbf{x}| = \sqrt{x^2 + y^2 + z^2}$ and denote

$$\partial_{\mathbf{n}} = \mathbf{n} \cdot \nabla = n_1 \partial_x + n_2 \partial_y + n_3 \partial_z, \qquad \partial_{\mathbf{nn}} = \partial_{\mathbf{n}} (\partial_{\mathbf{n}}). \tag{2.1}$$

Using the equality (see [28,30] and a mathematical proof in the Appendix A)

$$U_{\rm dip}(\mathbf{x}) = \frac{3}{4\pi r^3} \left(1 - \frac{3(\mathbf{x} \cdot \mathbf{n})^2}{r^2} \right) = -\delta(\mathbf{x}) - 3\partial_{\mathbf{nn}} \left(\frac{1}{4\pi r} \right), \qquad \mathbf{x} \in \mathbb{R}^3, \tag{2.2}$$

with $\delta(\mathbf{x})$ being the Dirac distribution function, it is straightforward to get the Fourier transform of $U_{\rm dip}(\mathbf{x})$ as

$$\widehat{(U_{\rm dip})}(\xi) = -1 + \frac{3(\mathbf{n} \cdot \xi)^2}{|\xi|^2}, \qquad \xi \in \mathbb{R}^3. \tag{2.3}$$

Introducing a new function

$$\varphi(\mathbf{x}, t) := \left(\frac{1}{4\pi |\mathbf{x}|} \right) * |\psi(\cdot, t)|^2 = \frac{1}{4\pi} \int_{\mathbb{R}^3} \frac{1}{|\mathbf{x} - \mathbf{x}'|} |\psi(\mathbf{x}', t)|^2 \, d\mathbf{x}', \qquad \mathbf{x} \in \mathbb{R}^3, \ t \geqslant 0, \tag{2.4}$$

we obtain

$$U_{\rm dip} * |\psi(\cdot,t)|^2 = -|\psi(\mathbf{x},t)|^2 - 3\tilde{\varphi}(\mathbf{x},t), \quad \mathbf{x}\in\mathbb{R}^3,\ t\geqslant 0, \tag{2.5}$$

with

$$\tilde{\varphi}(\mathbf{x},t) = \partial_{\mathbf{nn}}(\varphi(\mathbf{x},t)) = \left[\partial_{\mathbf{nn}}\left(\frac{1}{4\pi|\mathbf{x}|}\right)\right] * |\psi(\cdot,t)|^2 = \left(\frac{1}{4\pi|\mathbf{x}|}\right) * \left[\partial_{\mathbf{nn}}|\psi(\cdot,t)|^2\right]. \tag{2.6}$$

In fact, the above equality decouples the dipolar interaction potential into a short-range and a long-range interaction which correspond to the first and second terms in the right hand side of (2.5), respectively. Plugging (2.5) into (1.4) and noticing (2.4) and (2.6), we can reformulate the GPE (1.4) into a Gross–Pitaevskii–Poisson type system.

$$i\partial_t\psi(\mathbf{x},t) = \left[-\frac{1}{2}\nabla^2 + V(\mathbf{x}) + (\beta-\lambda)|\psi(\mathbf{x},t)|^2 - 3\lambda\tilde{\varphi}(\mathbf{x},t)\right]\psi(\mathbf{x},t), \quad \mathbf{x}\in\mathbb{R}^3,\ t>0, \tag{2.7}$$

$$\tilde{\varphi}(\mathbf{x},t) = \partial_{\mathbf{nn}}\varphi(\mathbf{x},t), \qquad -\nabla^2\varphi(\mathbf{x},t) = |\psi(\mathbf{x},t)|^2, \qquad \lim_{|\mathbf{x}|\to\infty}\varphi(\mathbf{x},t) = 0. \tag{2.8}$$

Note that the far-field condition in (2.8) makes the Poisson equation uniquely solvable. Using (2.8) and integration by parts, we can reformulate the energy functional $E(\cdot)$ in (1.7) as

$$E(\psi) = \int_{\mathbb{R}^3}\left[\frac{1}{2}|\nabla\psi|^2 + V(\mathbf{x})|\psi|^2 + \frac{1}{2}(\beta-\lambda)|\psi|^4 + \frac{3\lambda}{2}|\partial_{\mathbf{n}}\nabla\varphi|^2\right]d\mathbf{x}, \tag{2.9}$$

where φ is defined through (2.8). This immediately shows that the decoupled short-range and long-range interactions of the dipolar interaction potential are attractive and repulsive, respectively, when $\lambda>0$; and are repulsive and attractive, respectively, when $\lambda<0$. Similarly, the nonlinear eigenvalue problem (1.9) can be reformulated as

$$\mu\phi(\mathbf{x}) = \left[-\frac{1}{2}\nabla^2 + V(\mathbf{x}) + (\beta-\lambda)|\phi|^2 - 3\lambda\tilde{\varphi}(\mathbf{x})\right]\phi(\mathbf{x}), \tag{2.10}$$

$$\tilde{\varphi}(\mathbf{x}) = \partial_{\mathbf{nn}}\varphi(\mathbf{x}), \quad -\nabla^2\varphi(\mathbf{x}) = |\phi(\mathbf{x})|^2, \quad \mathbf{x}\in\mathbb{R}^3, \quad \lim_{|\mathbf{x}|\to\infty}\varphi(\mathbf{x}) = 0. \tag{2.11}$$

2.1. Existence and uniqueness for ground states

Under the new formulation for the energy functional $E(\cdot)$ in (2.9), we have.

Lemma 2.1. *For the energy $E(\cdot)$ in (2.9), we have*

(i) *For any $\phi\in S$, denote $\rho(\mathbf{x}) = |\phi(\mathbf{x})|^2$ for $\mathbf{x}\in\mathbb{R}^3$, then we have*

$$E(\phi) \geqslant E(|\phi|) = E(\sqrt{\rho}), \qquad \forall\phi\in S, \tag{2.12}$$

so the minimizer ϕ_g of (1.11) is of the form $e^{i\theta_0}|\phi_g|$ for some constant $\theta_0\in\mathbb{R}$.

(ii) *When $\beta\geqslant 0$ and $-\frac{1}{2}\beta\leqslant\lambda\leqslant\beta$, the energy $E(\sqrt{\rho})$ is strictly convex in ρ.*

Proof. For any $\phi\in S$, denote $\rho = |\phi|^2$ and consider the Poisson equation

$$\nabla^2\varphi(\mathbf{x}) = -|\phi(\mathbf{x})|^2 := -\rho(\mathbf{x}), \quad \mathbf{x}\in\mathbb{R}^3, \qquad \lim_{|\mathbf{x}|\to\infty}\varphi(\mathbf{x}) = 0. \tag{2.13}$$

Noticing (2.1) with $|\mathbf{n}| = 1$, we have the estimate

$$\|\partial_{\mathbf{n}}\nabla\varphi\|_2 \leqslant \|D^2\varphi\|_2 = \|\nabla^2\varphi\|_2 = \|\rho\|_2 = \|\phi\|_4^2, \qquad \text{with} \quad D^2 = \nabla\nabla. \tag{2.14}$$

(i) Write $\phi(\mathbf{x}) = e^{i\theta(\mathbf{x})}|\phi(\mathbf{x})|$, noticing (2.9) with $\psi = \phi$ and (2.13), we get

$$\begin{aligned} E(\phi) &= \int_{\mathbb{R}^3}\left[\frac{1}{2}|\nabla|\phi||^2 + \frac{1}{2}|\phi|^2|\nabla\theta(\mathbf{x})|^2 + V(\mathbf{x})|\phi|^2 + \frac{1}{2}(\beta-\lambda)|\phi|^4 + \frac{3\lambda}{2}|\partial_{\mathbf{n}}\nabla\varphi|^2\right]d\mathbf{x} \\ &\geqslant \int_{\mathbb{R}^3}\left[\frac{1}{2}|\nabla|\phi||^2 + V(\mathbf{x})|\phi|^2 + \frac{1}{2}(\beta-\lambda)|\phi|^4 + \frac{3\lambda}{2}|\partial_{\mathbf{n}}\nabla\varphi|^2\right]d\mathbf{x} = E(|\phi|) = E(\sqrt{\rho}), \qquad \forall\phi\in S, \end{aligned} \tag{2.15}$$

and the equality holds iff $\nabla\theta(\mathbf{x}) = 0$ for $\mathbf{x}\in\mathbb{R}^3$, which means $\theta(\mathbf{x})\equiv\theta_0$ is a constant.

(ii) From (2.9) with $\psi = \phi$ and noticing (2.13), we can split the energy $E(\sqrt{\rho})$ into two parts, i.e.

$$E(\sqrt{\rho}) = E_1(\sqrt{\rho}) + E_2(\sqrt{\rho}), \tag{2.16}$$

where

$$E_1(\sqrt{\rho}) = \int_{\mathbb{R}^3} \left[\frac{1}{2}|\nabla\sqrt{\rho}|^2 + V(\mathbf{x})\rho\right] d\mathbf{x}, \tag{2.17}$$

$$E_2(\sqrt{\rho}) = \int_{\mathbb{R}^3} \left[\frac{1}{2}(\beta-\lambda)|\rho|^2 + \frac{3\lambda}{2}|\partial_{\mathbf{n}}\nabla\varphi|^2\right] d\mathbf{x}. \tag{2.18}$$

As shown in [26], $E_1(\sqrt{\rho})$ is convex (strictly) in ρ. Thus we only need prove $E_2(\sqrt{\rho})$ is convex too. In order to do so, consider $\sqrt{\rho_1} \in S$, $\sqrt{\rho_2} \in S$, and let φ_1 and φ_2 be the solutions of the Poisson Eq. (2.13) with $\rho = \rho_1$ and $\rho = \rho_2$, respectively. For any $\alpha \in [0,1]$, we have $\sqrt{\alpha\rho_1 + (1-\alpha)\rho_2} \in S$, and

$$\alpha E_2(\sqrt{\rho_1}) + (1-\alpha)E_2(\sqrt{\rho_2}) - E_2\left(\sqrt{\alpha\rho_1 + (1-\alpha)\rho_2}\right) = \alpha(1-\alpha)\int_{\mathbb{R}^3}\left[\frac{1}{2}(\beta-\lambda)(\rho_1-\rho_2)^2 + \frac{3\lambda}{2}|\partial_{\mathbf{n}}\nabla(\varphi_1-\varphi_2)|^2\right] d\mathbf{x}, \tag{2.19}$$

which immediately implies that $E_2(\sqrt{\rho})$ is convex if $\beta \geqslant 0$ and $0 \leqslant \lambda \leqslant \beta$. If $\beta \geqslant 0$ and $-\frac{1}{2}\beta \leqslant \lambda < 0$, noticing that $\alpha\varphi_1 + (1-\alpha)\varphi_2$ is the solution of the Poisson Eq. (2.13) with $\rho = \alpha\rho_1 + (1-\alpha)\rho_2$, combining (2.14) with $\varphi = \varphi_1 - \varphi_2$ and (2.19), we obtain $E_2(\sqrt{\rho})$ is convex again. Combining all the results above together, the conclusion follows. □

Now, we are able to prove the existence and uniqueness as well as nonexistence results for the ground state of a dipolar BEC in different parameter regimes.

Theorem 2.1. *Assume $V(\mathbf{x}) \geqslant 0$ for $\mathbf{x} \in \mathbb{R}^3$ and $\lim_{|\mathbf{x}|\to\infty} V(\mathbf{x}) = \infty$ (i.e., confining potential), then we have:*

(i) *If $\beta \geqslant 0$ and $-\frac{1}{2}\beta \leqslant \lambda \leqslant \beta$, there exists a ground state $\phi_g \in S$, and the positive ground state $|\phi_g|$ is unique. Moreover, $\phi_g = e^{i\theta_0}|\phi_g|$ for some constant $\theta_0 \in \mathbb{R}$.*

(ii) *If $\beta < 0$, or $\beta \geqslant 0$ and $\lambda < -\frac{1}{2}\beta$ or $\lambda > \beta$, there exists no ground state, i.e., $\inf_{\phi\in S} E(\phi) = -\infty$.*

Proof.

(i) Assume $\beta \geqslant 0$ and $-\frac{1}{2}\beta \leqslant \lambda \leqslant \beta$, we first show $E(\phi)$ is nonnegative in S, i.e.

$$E(\phi) = \int_{\mathbb{R}^3}\left[\frac{1}{2}|\nabla\phi|^2 + V(\mathbf{x})|\phi|^2 + \frac{1}{2}(\beta-\lambda)|\phi|^4 + \frac{3\lambda}{2}|\partial_{\mathbf{n}}\nabla\varphi|^2\right] d\mathbf{x} \geqslant 0, \qquad \forall\phi \in S. \tag{2.20}$$

In fact, when $\beta \geqslant 0$ and $0 \leqslant \lambda \leqslant \beta$, noticing (2.9) with $\psi = \phi$, it is obvious that (2.20) is valid. When $\beta \geqslant 0$ and $-\frac{1}{2}\beta \leqslant \lambda < 0$, combining (2.9) with $\psi = \phi$, (2.13) and (2.14), we obtain (2.20) again as

$$\begin{aligned} E(\phi) &\geqslant \int_{\mathbb{R}^3}\left[\frac{1}{2}|\nabla\phi|^2 + V(\mathbf{x})|\phi|^2 + \frac{1}{2}(\beta-\lambda)|\phi|^4 + \frac{3\lambda}{2}|\phi|^4\right] d\mathbf{x} = \int_{\mathbb{R}^3}\left[\frac{1}{2}|\nabla\phi|^2 + V(\mathbf{x})|\phi|^2 + \frac{1}{2}(\beta+2\lambda)|\phi|^4\right] d\mathbf{x} \\ &\geqslant 0. \end{aligned} \tag{2.21}$$

Now, let $\{\phi^n\}_{n=0}^{\infty} \subset S$ be a minimizing sequence of the minimization problem (1.11). Then there exists a constant C such that

$$\|\nabla\phi^n\|_2 \leqslant C, \qquad \|\phi^n\|_4 \leqslant C, \qquad \int_{\mathbb{R}^3} V(\mathbf{x})|\phi^n(\mathbf{x})|^2 d\mathbf{x} \leqslant C, \qquad n \geqslant 0. \tag{2.22}$$

Therefore ϕ^n belongs to a weakly compact set in L^4, $H^1 = \{\phi \,|\, \|\phi\|_2 + \|\nabla\phi\|_2 < \infty\}$, and $L^2_V = \{\phi \mid \int_{\mathbb{R}^3} V(\mathbf{x})|\phi(\mathbf{x})|^2 \, d\mathbf{x} < \infty\}$ with a weighted L^2-norm given by $\|\phi\|_V = [\int_{\mathbb{R}^3} |\phi(\mathbf{x})|^2 V(\mathbf{x}) d\mathbf{x}]^{1/2}$. Thus, there exists a $\phi^\infty \in H^1 \cap L^2_V \cap L^4$ and a subsequence (which we denote as the original sequence for simplicity), such that

$$\phi^n \rightharpoonup \phi^\infty, \quad \text{in } L^2 \cap L^4 \cap L^2_V, \qquad \nabla\phi^n \rightharpoonup \nabla\phi^\infty, \quad \text{in } L^2. \tag{2.23}$$

Also, we can suppose that ϕ^n is nonnegative, since we can replace them with $|\phi^n|$, which also minimize the functional E. Similar as in [26], we can obtain $\|\phi^\infty\|_2 = 1$ due to the confining property of the potential $V(\mathbf{x})$. So, $\phi^\infty \in S$. Moreover, the L^2-norm convergence of ϕ^n and weak convergence in (2.23) would imply the strong convergence $\phi^n \to \phi^\infty \in L^2$. Thus, employing Hölder inequality and Sobolev inequality, we obtain

$$\|(\phi^n)^2 - (\phi^\infty)^2\|_2 \leqslant C_1\|\phi^n - \phi^\infty\|_2^{1/2}\left(\|\phi^n\|_6^{1/2} + \|\phi^\infty\|_6^{1/2}\right) \leqslant C_2\left(\|\nabla\phi^n\|_2^{1/2} + \|\nabla\phi^\infty\|_2^{1/2}\right)\|\phi^n - \phi^\infty\|_2 \to 0, \qquad n \to \infty, \tag{2.24}$$

which shows $\rho^n = (\phi^n)^2 \to \rho^\infty = (\phi^\infty)^2 \in L^2$. Since $E_2(\sqrt{\rho})$ in (2.18) is convex and lower semi-continuous in ρ, thus $E_2(\phi^\infty) \leqslant \lim_{n\to\infty} E_2(\phi^n)$. For E_1 in (2.17), $E_1(\phi^\infty) \leqslant \lim_{n\to\infty} E_1(\phi^n)$ because of the lower semi-continuity of the H^1- and L^2_V-norm. Combining the results together, we know $E(\phi^\infty) \leqslant \lim_{n\to\infty} E(\phi^n)$, which proves that ϕ^∞ is indeed a minimizer of the minimization problem (1.11). The uniqueness follows from the strictly convexity of $E(\sqrt{\rho})$ as shown in Lemma 2.1.

(ii) Assume $\beta < 0$, or $\beta \geqslant 0$ and $\lambda < -\frac{1}{2}\beta$ or $\lambda > \beta$. Without loss of generality, we assume $\mathbf{n} = (0,0,1)^T$ and choose the function

$$\phi_{\varepsilon_1,\varepsilon_2}(\mathbf{x}) = \frac{1}{(2\pi\varepsilon_1)^{1/2}}\cdot\frac{1}{(2\pi\varepsilon_2)^{1/4}}\exp\left(-\frac{x^2+y^2}{2\varepsilon_1}\right)\exp\left(-\frac{z^2}{2\varepsilon_2}\right), \qquad \mathbf{x}\in\mathbb{R}^3, \tag{2.25}$$

with ε_1 and ε_2 two small positive parameters (in fact, for general $\mathbf{n}\in\mathbb{R}^3$ satisfying $|\mathbf{n}| = 1$, we can always choose $0\neq\mathbf{n}_1\in\mathbb{R}^3$ and $0\neq\mathbf{n}_2\in\mathbb{R}^3$ such that $\{\mathbf{n}_1,\mathbf{n}_2,\mathbf{n}\}$ forms an orthonormal basis of $\mathbb{R}^3$ and do the change of variables $\mathbf{x} = (x,y,z)^T$ to $\mathbf{y} = (\mathbf{x}\cdot\mathbf{n}_1,\mathbf{x}\cdot\mathbf{n}_2,\mathbf{x}\cdot\mathbf{n})^T$ on the right hand side of (2.9), the following computation is still valid). Taking the standard Fourier transform at both sides of the Poisson equation

$$-\nabla^2\varphi_{\varepsilon_1,\varepsilon_2}(\mathbf{x}) = |\phi_{\varepsilon_1,\varepsilon_2}(\mathbf{x})|^2 = \rho_{\varepsilon_1,\varepsilon_2}(\mathbf{x}), \quad \mathbf{x}\in\mathbb{R}^3, \qquad \lim_{|\mathbf{x}|\to\infty}\varphi_{\varepsilon_1,\varepsilon_2}(\mathbf{x}) = 0, \tag{2.26}$$

we get

$$|\xi|^2\widehat{\varphi_{\varepsilon_1,\varepsilon_2}}(\xi) = \widehat{\rho_{\varepsilon_1,\varepsilon_2}}(\xi), \qquad \xi\in\mathbb{R}^3. \qquad \square \tag{2.27}$$

Using the Plancherel formula and changing of variables, we obtain

$$\begin{aligned}\|\partial_{\mathbf{n}}\nabla\varphi_{\varepsilon_1,\varepsilon_2}\|_2^2 &= \frac{1}{(2\pi)^3}\|(\mathbf{n}\cdot\xi)\widehat{\varphi_{\varepsilon_1,\varepsilon_2}}(\xi)\|_2^2 = \frac{1}{(2\pi)^3}\int_{\mathbb{R}^3}\frac{|\xi_3|^2}{|\xi|^2}\left|\widehat{\rho_{\varepsilon_1,\varepsilon_2}}(\xi)\right|^2 d\xi\\ &= \frac{1}{(2\pi)^3\varepsilon_1\sqrt{\varepsilon_2}}\int_{\mathbb{R}^3}\frac{|\xi_3|^2}{(|\xi_1|^2+|\xi_2|^2)\cdot\frac{\varepsilon_2}{\varepsilon_1}+|\xi_3|^2}\left|\widehat{\rho_{1,1}}(\xi)\right|^2 d\xi, \quad \varepsilon_1,\varepsilon_2>0.\end{aligned} \tag{2.28}$$

By the dominated convergence theorem with fixed $\varepsilon_1\sqrt{\varepsilon_2}$, we get

$$\|\partial_{\mathbf{n}}\nabla\varphi_{\varepsilon_1,\varepsilon_2}\|_2^2 \to \begin{cases} 0, & \varepsilon_2/\varepsilon_1\to+\infty,\\ \frac{1}{(2\pi)^3\varepsilon_1\sqrt{\varepsilon_2}}\int_{\mathbb{R}^3}\left|\widehat{\rho_{1,1}}(\xi)\right|^2 d\xi = \|\rho_{\varepsilon_1,\varepsilon_2}\|_2^2 = \|\phi_{\varepsilon_1,\varepsilon_2}\|_4^4, & \varepsilon_2/\varepsilon_1\to 0^+.\end{cases} \tag{2.29}$$

When fixed $\varepsilon_1\sqrt{\varepsilon_2}$, the last integral in (2.28) is continuous in $\varepsilon_2/\varepsilon_1 > 0$. Thus, for any $\alpha\in(0,1)$, by adjusting $\varepsilon_2/\varepsilon_1$: $= C_\alpha > 0$, we could have $\|\partial_{\mathbf{n}}\nabla\varphi_{\varepsilon_1,\varepsilon_2}\|_2^2 = \alpha\|\phi_{\varepsilon_1,\varepsilon_2}\|_4^4$. Substituting (2.25) into (2.17) and (2.18) with $\sqrt{\rho} = \phi_{\varepsilon_1,\varepsilon_2}$ under fixed $\varepsilon_2/\varepsilon_1 > 0$, we get

$$E_1(\phi_{\varepsilon_1,\varepsilon_2}) = \int_{\mathbb{R}^3}\left[\frac{1}{2}|\nabla\phi_{\varepsilon_1,\varepsilon_2}|^2 + V(\mathbf{x})|\phi_{\varepsilon_1,\varepsilon_2}|^2\right]d\mathbf{x} = \frac{C_1}{\varepsilon_1}+\frac{C_2}{\varepsilon_2}+\mathcal{O}(1), \tag{2.30}$$

$$E_2(\phi_{\varepsilon_1,\varepsilon_2}) = \frac{1}{2}\int_{\mathbb{R}^3}(\beta-\lambda+3\alpha\lambda))|\phi_{\varepsilon_1,\varepsilon_2}|^4 d\mathbf{x} = \frac{\beta-\lambda+3\alpha\lambda}{2}\cdot\frac{C_3}{\varepsilon_1\sqrt{\varepsilon_2}}, \tag{2.31}$$

with some constants $C_1, C_2, C_3 > 0$ independent of ε_1 and ε_2. Thus, if $\beta < 0$, choose $\alpha = 1/3$; if $\beta\geqslant 0$ and $\lambda < -\frac{1}{2}\beta$, choose $1/3 - \frac{\beta}{3\lambda} < \alpha < 1$; and if $\beta\geqslant 0$ and $\lambda > \beta$, choose $0 < \alpha < \frac{1}{3}(1-\frac{\beta}{\lambda})$; as $\varepsilon_1, \varepsilon_2\to 0^+$, we can get $\inf_{\phi\in S}E(\phi) = \lim_{\varepsilon_1,\varepsilon_2\to 0^+}E_1(\phi_{\varepsilon_1,\varepsilon_2}) + E_2(\phi_{\varepsilon_1,\varepsilon_2}) = -\infty$, which implies that there exists no ground state of the minimization problem (1.11). □

By splitting the total energy $E(\cdot)$ in (2.9) into kinetic, potential, interaction and dipolar energies, i.e.

$$E(\phi) = E_{\text{kin}}(\phi) + E_{\text{pot}}(\phi) + E_{\text{int}}(\phi) + E_{\text{dip}}(\phi), \tag{2.32}$$

where

$$\begin{aligned}E_{\text{kin}}(\phi) &= \frac{1}{2}\int_{\mathbb{R}^3}|\nabla\phi(\mathbf{x})|^2 d\mathbf{x},\ E_{\text{pot}}(\phi) = \int_{\mathbb{R}^3}V(\mathbf{x})|\phi(\mathbf{x})|^2 d\mathbf{x},\ E_{\text{int}}(\phi) = \frac{\beta}{2}\int_{\mathbb{R}^3}|\phi(\mathbf{x})|^4 d\mathbf{x},\\ E_{\text{dip}}(\phi) &= \frac{\lambda}{2}\int_{\mathbb{R}^3}\left(U_{\text{dip}}*|\phi|^2\right)|\phi(\mathbf{x})|^2 d\mathbf{x} = \frac{\lambda}{2}\int_{\mathbb{R}^3}|\phi(\mathbf{x})|^2\left[-|\phi(\mathbf{x})|^2 - 3\partial_{\mathbf{nn}}\varphi\right]d\mathbf{x}\\ &= \frac{\lambda}{2}\int_{\mathbb{R}^3}\left[-|\phi(\mathbf{x})|^4 + 3(\nabla^2\varphi)(\partial_{\mathbf{nn}}\varphi)\right]d\mathbf{x} = \frac{\lambda}{2}\int_{\mathbb{R}^3}\left[-|\phi(\mathbf{x})|^4 + 3|\partial_{\mathbf{n}}\nabla\varphi|^2\right]d\mathbf{x},\end{aligned} \tag{2.33}$$

with φ defined in (2.11), we have the following Viral identity:

Proposition 2.2. *Suppose ϕ_e is a stationary state of a dipolar BEC, i.e. an eigenfunction of the nonlinear eigenvalue problem (1.9) under the constraint (1.10), then we have*

$$2E_{\text{kin}}(\phi_e) - 2E_{\text{trap}}(\phi_e) + 3E_{\text{int}}(\phi_e) + 3E_{\text{dip}}(\phi_e) = 0. \tag{2.34}$$

Proof. Follow the analogous proof for a BEC without dipolar interaction [31] and we omit the details here for brevity. □

2.2. Analytical results for dynamics

The well-posedness of the Cauchy problem of (1.1) was discussed in [12] by analyzing the convolution kernel $U_{\text{dip}}(\mathbf{x})$ with detailed Fourier transform. Under the new formulation (2.7) and (2.8), here we present a simpler proof for the well-posedness and show finite time blow-up for the Cauchy problem of a dipolar BEC in different parameter regimes. Denote

$$X = \left\{ u \in H^1(\mathbb{R}^3) \ | \|u\|_X^2 = \|u\|_{L^2}^2 + \|\nabla u\|_{L^2}^2 + \int_{\mathbb{R}^3} V(\mathbf{x})|u(\mathbf{x})|^2 \, d\mathbf{x} < \infty \right\}.$$

Theorem 2.3. *(Well-posedness) Suppose the real-valued trap potential $V(\mathbf{x}) \in C^\infty(\mathbb{R}^3)$ such that $V(\mathbf{x}) \geqslant 0$ for $\mathbf{x} \in \mathbb{R}^3$ and $D^\alpha V(\mathbf{x}) \in L^\infty(\mathbb{R}^3)$ for all $\alpha \in \mathbb{N}_0^3$ with $|\alpha| \geqslant 2$. For any initial data $\psi(\mathbf{x}, t=0) = \psi_0(\mathbf{x}) \in X$, there exists $T_{\max} \in (0, +\infty]$ such that the problem (2.7) and (2.8) has a unique maximal solution $\psi \in C([0, T_{\max}), X)$. It is maximal in the sense that if $T_{\max} < \infty$, then $\|\psi(\cdot,t)\|_X \to \infty$ when $t \to T_{\max}^-$. Moreover, the mass $N(\psi(\cdot,t))$ and energy $E(\psi(\cdot,t))$ defined in (1.6) and (1.7), respectively, are conserved for $t \in [0, T_{max})$. Specifically, if $\beta \geqslant 0$ and $-\frac{1}{2}\beta \leqslant \lambda \leqslant \beta$, the solution to (2.7) and (2.8) is global in time, i.e., $T_{\max} = \infty$.*

Proof. For any $\phi \in X$, let φ be the solution of the Poisson Eq. (2.13), denote $\rho = |\phi|^2$ and define

$$G(\phi, \bar{\phi}) := G(\rho) = \frac{1}{2} \int_{\mathbb{R}^3} |\phi(\mathbf{x})|^2 \partial_{\mathbf{nn}} \varphi(\mathbf{x}) \, d\mathbf{x}, \qquad g(\phi) = \frac{\delta G(\phi, \bar{\phi})}{\delta \bar{\phi}} = \phi \ \partial_{\mathbf{nn}} \varphi, \tag{2.35}$$

where $\bar{f}$ denotes the conjugate of f. Noticing (2.14), it is easy to show that $G(\phi) \in C^1(X, \mathbb{R})$, $g(\phi) \in C(X, L^p)$ for some $p \in (6/5, 2]$, and

$$\|g(u) - g(v)\|_{L^p} \leqslant C(\|u\|_X + \|v\|_X)\|u - v\|_{L^r}, \quad \text{for some } r \in [2, 6), \qquad \forall u, v \in X. \tag{2.36}$$

Applying the standard Theorems 9.2.1, 4.12.1 and 5.7.1 in [13,40] for the well-posedness of the nonlinear Schrödinger equation, we can obtain the results immediately. □

Theorem 2.4. *(Finite time blow-up) Let $\beta < 0$, or $\beta \geqslant 0$ and $\lambda < -\frac{1}{2}\beta$ or $\lambda > \beta$, and assume $V(\mathbf{x})$ satisfies $3V(\mathbf{x}) + \mathbf{x}\cdot\nabla V(\mathbf{x}) \geqslant 0$ for $\mathbf{x} \in \mathbb{R}^3$. Given any initial data $\psi(\mathbf{x}, t=0) = \psi_0(\mathbf{x}) \in X$ for the problem (2.7) and (2.8), there exists finite time blow-up, i.e., $T_{max} < \infty$, if one of the following holds:*

(i) $E(\psi_0) < 0$;
(ii) $E(\psi_0) = 0$ and Im $(\int_{\mathbb{R}^3} \bar{\psi}_0(\mathbf{x}) \ (\mathbf{x} \cdot \nabla \psi_0(\mathbf{x})) \, d\mathbf{x}) < 0$;
(iii) $E(\psi_0) > 0$ and Im $(\int_{\mathbb{R}^3} \bar{\psi}_0(\mathbf{x}) \ (\mathbf{x} \cdot \nabla \psi_0(\mathbf{x})) \, d\mathbf{x}) < -\sqrt{3E(\psi_0)}\|\mathbf{x}\psi_0\|_{L^2}$;

Table 1
Comparison for evaluating dipolar energy under different mesh sizes h.

	Case I		Case II		Case III	
	DST	DFT	DST	DFT	DST	DFT
$M = 32$ & $h = 1$	2.756E−2	2.756E−2	3.555E−18	1.279E−4	0.1018	0.1020
$M = 64$ & $h = 0.5$	1.629E−3	1.614E−3	9.154E−18	1.278E−4	9.788E−5	2.269E−4
$M = 128$ & $h = 0.25$	1.243E−7	1.588E−5	7.454E−17	1.278E−4	6.406E−7	1.284E−4

Table 2
Different quantities of the ground states of a dipolar BEC for $\beta = 0.20716N$ and $\lambda = 0.033146N$ with different number of particles N.

$\frac{N}{1000}$	E^g	μ^g	E^g_{kin}	E^g_{pot}	E^g_{int}	E^g_{dip}	σ^g_x	σ^g_z	$\rho_g(\mathbf{0})$
0.1	1.567	1.813	0.477	0.844	0.262	−0.015	0.796	1.299	0.06139
0.5	2.225	2.837	0.349	1.264	0.659	−0.047	0.940	1.745	0.02675
1	2.728	3.583	0.296	1.577	0.925	−0.070	1.035	2.009	0.01779
5	4.745	6.488	0.195	2.806	1.894	−0.151	1.354	2.790	0.00673
10	6.147	8.479	0.161	3.654	2.536	−0.204	1.538	3.212	0.00442
50	11.47	15.98	0.101	6.853	4.909	−0.398	2.095	4.441	0.00168
100	15.07	21.04	0.082	9.017	6.498	−0.526	2.400	5.103	0.00111

Table 3
Different quantities of the ground states of a dipolar BEC with different values of $\frac{\lambda}{\beta}$ with $\beta = 207.16$.

$\frac{\lambda}{\beta}$	E^g	μ^g	E^g_{kin}	E^g_{pot}	E^g_{int}	E^g_{dip}	σ^g_x	σ^g_z	$\rho_g(\mathbf{0})$
-0.5	2.957	3.927	0.265	1.721	0.839	0.131	1.153	1.770	0.01575
-0.25	2.883	3.817	0.274	1.675	0.853	0.081	1.111	1.879	0.01605
0	2.794	3.684	0.286	1.618	0.890	0.000	1.066	1.962	0.01693
0.25	2.689	3.525	0.303	1.550	0.950	−0.114	1.017	2.030	0.01842
0.5	2.563	3.332	0.327	1.468	1.047	−0.278	0.960	2.089	0.02087
0.75	2.406	3.084	0.364	1.363	1.212	−0.534	0.889	2.141	0.02536
1.0	2.193	2.726	0.443	1.217	1.575	−1.041	0.786	2.189	0.03630

where Im *(f) denotes the imaginary part of f.*

Proof. Define the variance

$$\sigma_V(t) := \sigma_V(\psi(\cdot,t)) = \int_{\mathbb{R}^3} |\mathbf{x}|^2 |\psi(\mathbf{x},t)|^2 \, d\mathbf{x} = \delta_x(t) + \delta_y(t) + \delta_z(t), \qquad t \geqslant 0, \tag{2.37}$$

where

$$\sigma_\alpha(t) := \sigma_\alpha(\psi(\cdot,t)) = \int_{\mathbb{R}^3} \alpha^2 |\psi(\mathbf{x},t)|^2 \, d\mathbf{x}, \qquad \alpha = x,\ y,\ z. \tag{2.38}$$

For $\alpha = x$, or y or z, differentiating (2.38) with respect to t, noticing (2.7) and (2.8), integrating by parts, we get

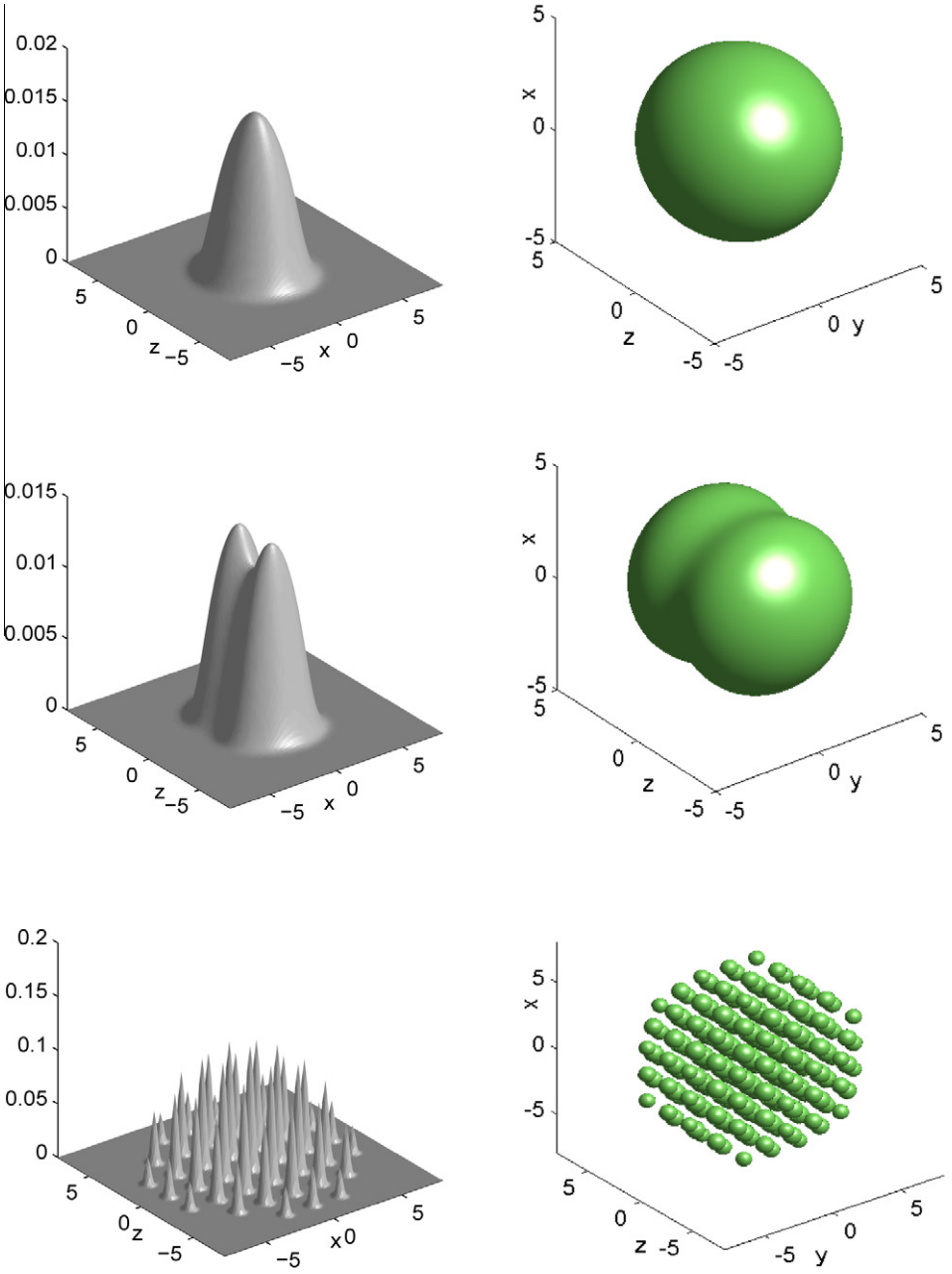

Fig. 1. Surface plots of $|\phi_g(x,0,z)|^2$ (left column) and isosurface plots of $|\phi_g(x,y,z)| = 0.01$ (right column) for the ground state of a dipolar BEC with $\beta = 401.432$ and $\lambda = 0.16\beta$ for harmonic potential (top row), double-well potential (middle row) and optical lattice potential (bottom row).

$$\frac{d}{dt}\sigma_\alpha(t) = -i\int_{\mathbb{R}^3}\left[\alpha\bar{\psi}(\mathbf{x},t)\partial_\alpha\psi(\mathbf{x},t) - \alpha\psi(\mathbf{x},t)\partial_\alpha\bar{\psi}(\mathbf{x},t)\right]d\mathbf{x}, \qquad t \geqslant 0. \tag{2.39}$$

Similarly, we have

$$\frac{d^2}{dt^2}\sigma_\alpha(t) = \int_{\mathbb{R}^3}\left[2|\partial_\alpha\psi|^2 + (\beta-\lambda)|\psi|^4 + 6\lambda|\psi|^2\alpha\partial_\alpha\partial_{\mathbf{nn}}\varphi - 2\alpha|\psi|^2\partial_\alpha V(\mathbf{x})\right]d\mathbf{x}. \tag{2.40}$$

Noticing (2.8) and

$$-\int_{\mathbb{R}^3}\nabla^2\varphi(\mathbf{x}\cdot\nabla\partial_{\mathbf{nn}}\varphi)\,d\mathbf{x} = \frac{3}{2}\int_{\mathbb{R}^3}|\partial_{\mathbf{n}}\nabla\varphi|^2\,d\mathbf{x},$$

summing (2.40) for $\alpha = x$, y and z, using (2.37) and (1.7), we get

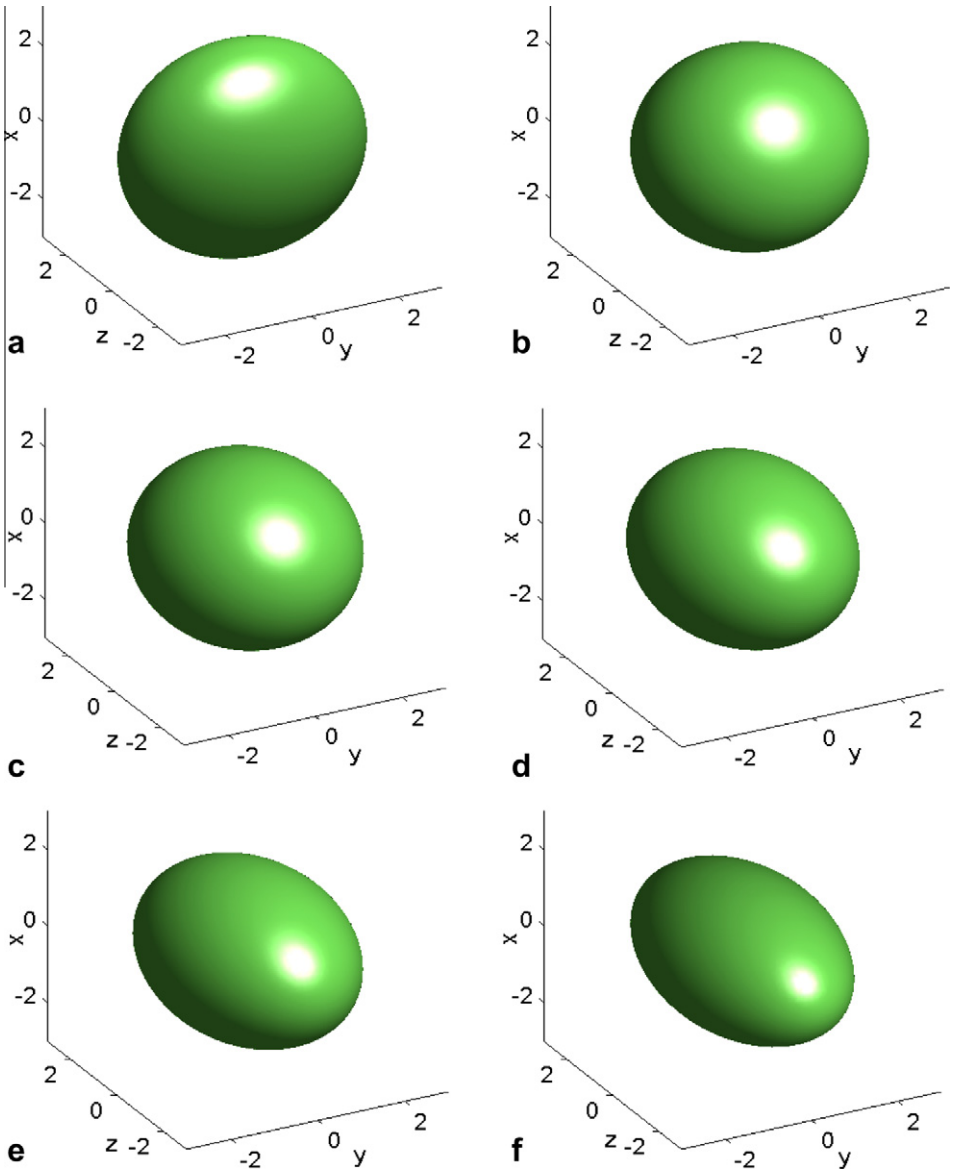

Fig. 2. Isosurface plots of the ground state $|\phi_g(\mathbf{x})| = 0.08$ of a dipolar BEC with the harmonic potential $V(\mathbf{x}) = \frac{1}{2}(x^2+y^2+z^2)$ and $\beta = 207.16$ for different values of $\frac{\lambda}{\beta}$: (a) $\frac{\lambda}{\beta} = -0.5$; (b) $\frac{\lambda}{\beta} = 0$; (c) $\frac{\lambda}{\beta} = 0.25$; (d) $\frac{\lambda}{\beta} = 0.5$; (e) $\frac{\lambda}{\beta} = 0.75$; (f) $\frac{\lambda}{\beta} = 1$.

$$\frac{d^2}{dt^2}\sigma_V(t) = 2\int_{\mathbb{R}^3}\left(|\nabla\psi|^2 + \frac{3}{2}(\beta-\lambda)|\psi|^4 + \frac{9}{2}\lambda|\partial_{\mathbf{n}}\nabla\psi|^2 - |\psi|^2(\mathbf{x}\cdot\nabla V(\mathbf{x}))\right)d\mathbf{x}$$
$$= 6E(\psi) - \int_{\mathbb{R}^3}|\nabla\psi(\mathbf{x},t)|^2 - 2\int_{\mathbb{R}^3}|\psi(\mathbf{x},t)|^2(3V(\mathbf{x}) + \mathbf{x}\cdot\nabla V(\mathbf{x}))\,d\mathbf{x} \leqslant 6E(\psi) \equiv 6E(\psi_0), \qquad t \geqslant 0. \tag{2.41}$$

Thus,

$$\sigma_V(t) \leqslant 3E(\psi_0)t^2 + \sigma_V'(0)t + \sigma_V(0), \qquad t \geqslant 0,$$

and the conclusion follows in the same manner as those in [40,13] for the standard nonlinear Schrödinger equation. □

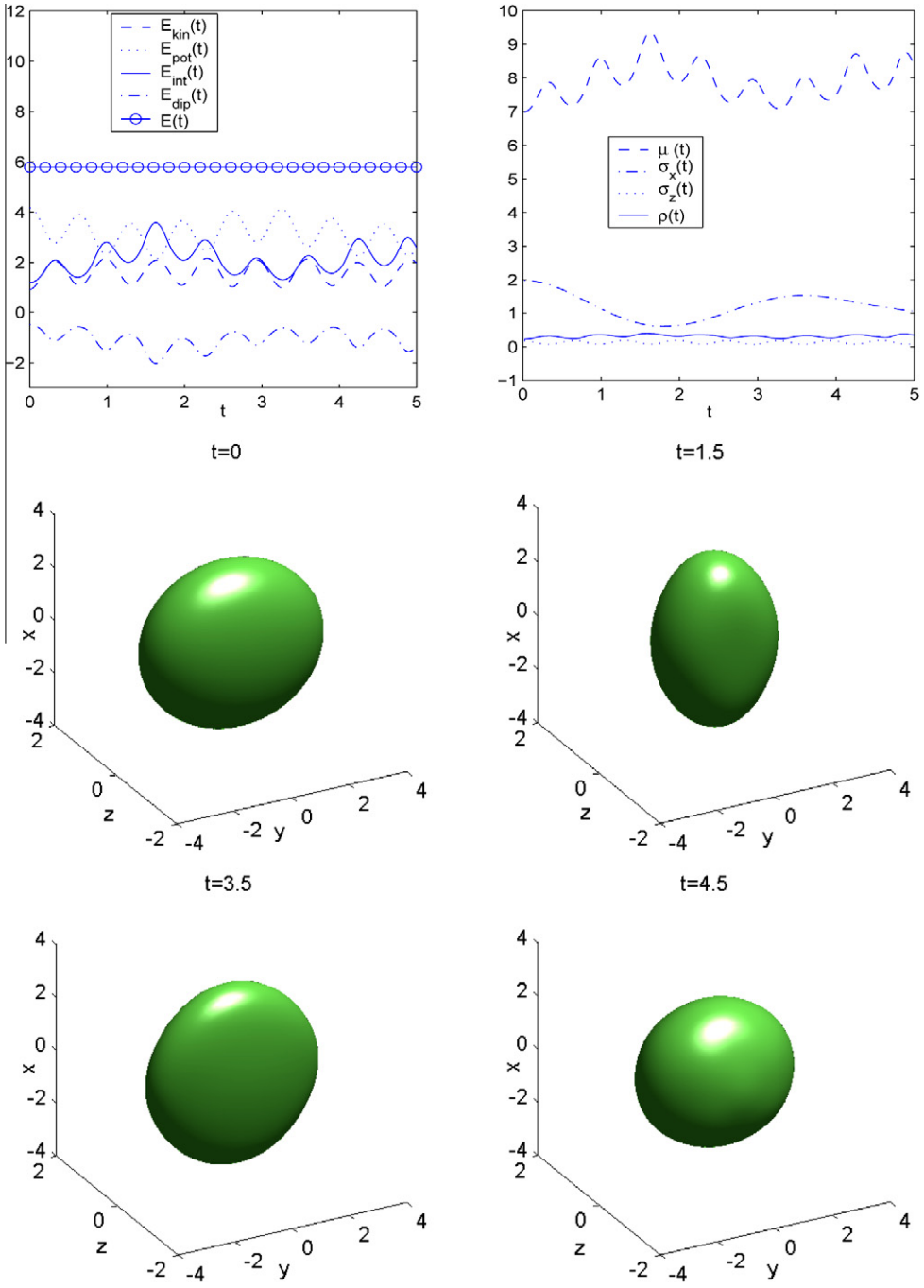

Fig. 3. Time evolution of different quantities and isosurface plots of the density function $\rho(\mathbf{x},t)$: = $|\psi(\mathbf{x},t)|^2$ = 0.01 at different times for a dipolar BEC when the dipolar direction is suddenly changed from $\mathbf{n} = (0,0,1)^T$ to $(1,0,0)^T$ at time $t = 0$.

3. A numerical method for computing ground states

Based on the new mathematical formulation for the energy in (2.9), we will present an efficient and accurate backward Euler sine pseudospectral method for computing the ground states of a dipolar BEC.

In practice, the whole space problem is usually truncated into a bounded computational domain $\Omega = [a,b] \times [c,d] \times [e,f]$ with homogeneous Dirichlet boundary condition. Various numerical methods have been proposed in the literatures for computing the ground states of BEC (see [37,15,4,3,7,14,11] and references therein). One of the popular and efficient techniques for dealing with the constraint (1.10) is through the following construction [4,8,3]: Choose a time step $\Delta t > 0$ and set $t_n = n\Delta t$ for $n = 0, 1, \ldots$ Applying the steepest decent method to the energy functional $E(\phi)$ in (2.9) without the constraint (1.10), and

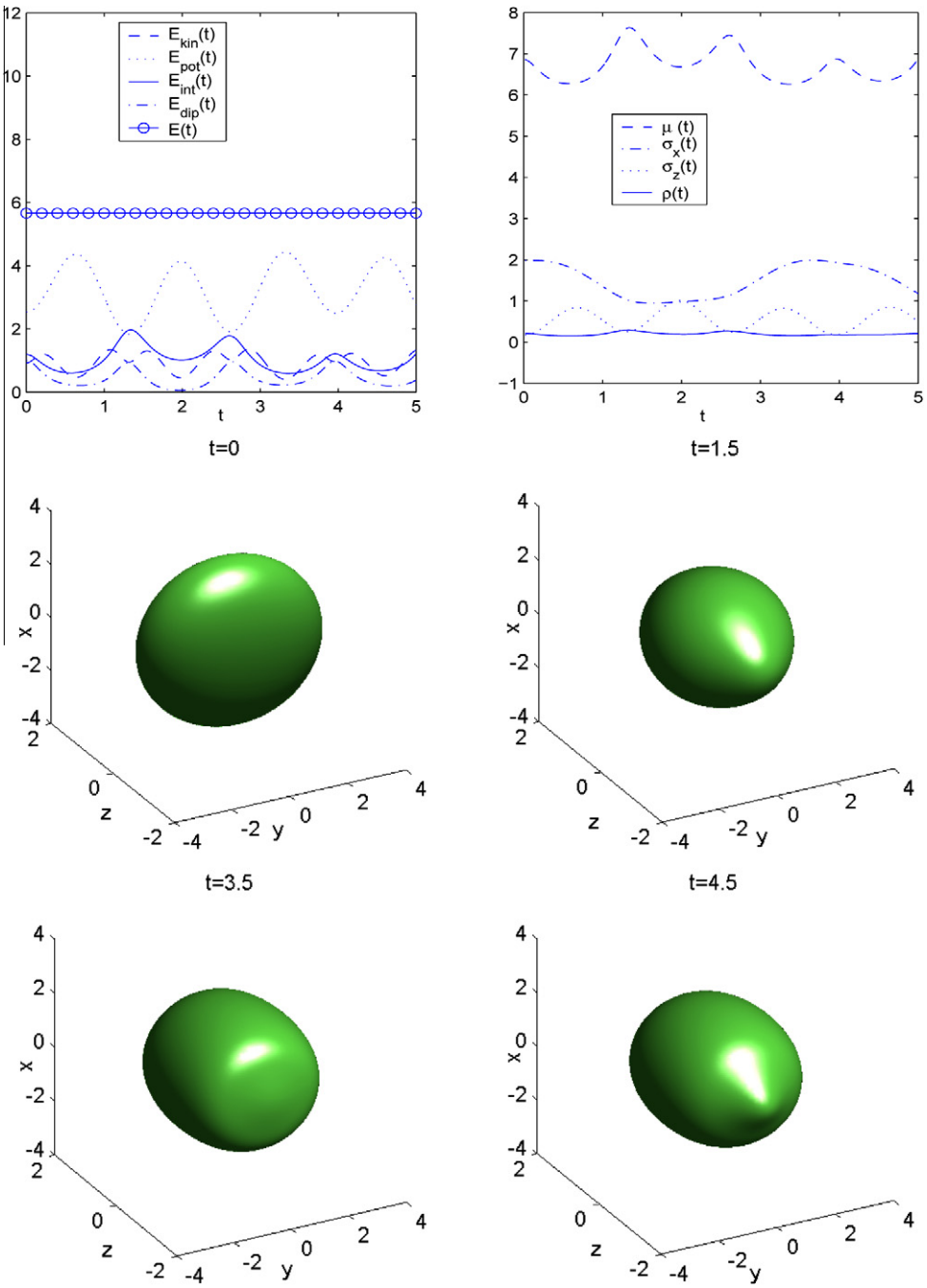

Fig. 4. Time evolution of different quantities and isosurface plots of the density function $\rho(\mathbf{x},t)$: $= |\psi(\mathbf{x},t)|^2 = 0.01$ at different times for a dipolar BEC when the trap potential is suddenly changed from from $\frac{1}{2}(x^2+y^2+25z^2)$ to $\frac{1}{2}(x^2+y^2+\frac{25}{4}z^2)$ at time $t = 0$.

then projecting the solution back to the unit sphere S at the end of each time interval $[t_n, t_{n+1}]$ in order to satisfy the constraint (1.10). This procedure leads to the function $\phi(\mathbf{x},t)$ is the solution of the following gradient flow with discrete normalization:

$$\partial_t \phi(\mathbf{x},t) = \left[\frac{1}{2}\nabla^2 - V(\mathbf{x}) - (\beta-\lambda)|\phi(\mathbf{x},t)|^2 + 3\lambda\tilde{\varphi}(\mathbf{x},t)\right]\phi(\mathbf{x},t), \tag{3.1}$$

$$\tilde{\varphi}(\mathbf{x},t) = \partial_{\mathbf{nn}}\varphi(\mathbf{x},t), \qquad -\nabla^2\varphi(\mathbf{x},t) = |\phi(\mathbf{x},t)|^2, \qquad \mathbf{x}\in\Omega,\ t_n \leqslant t < t_{n+1}, \tag{3.2}$$

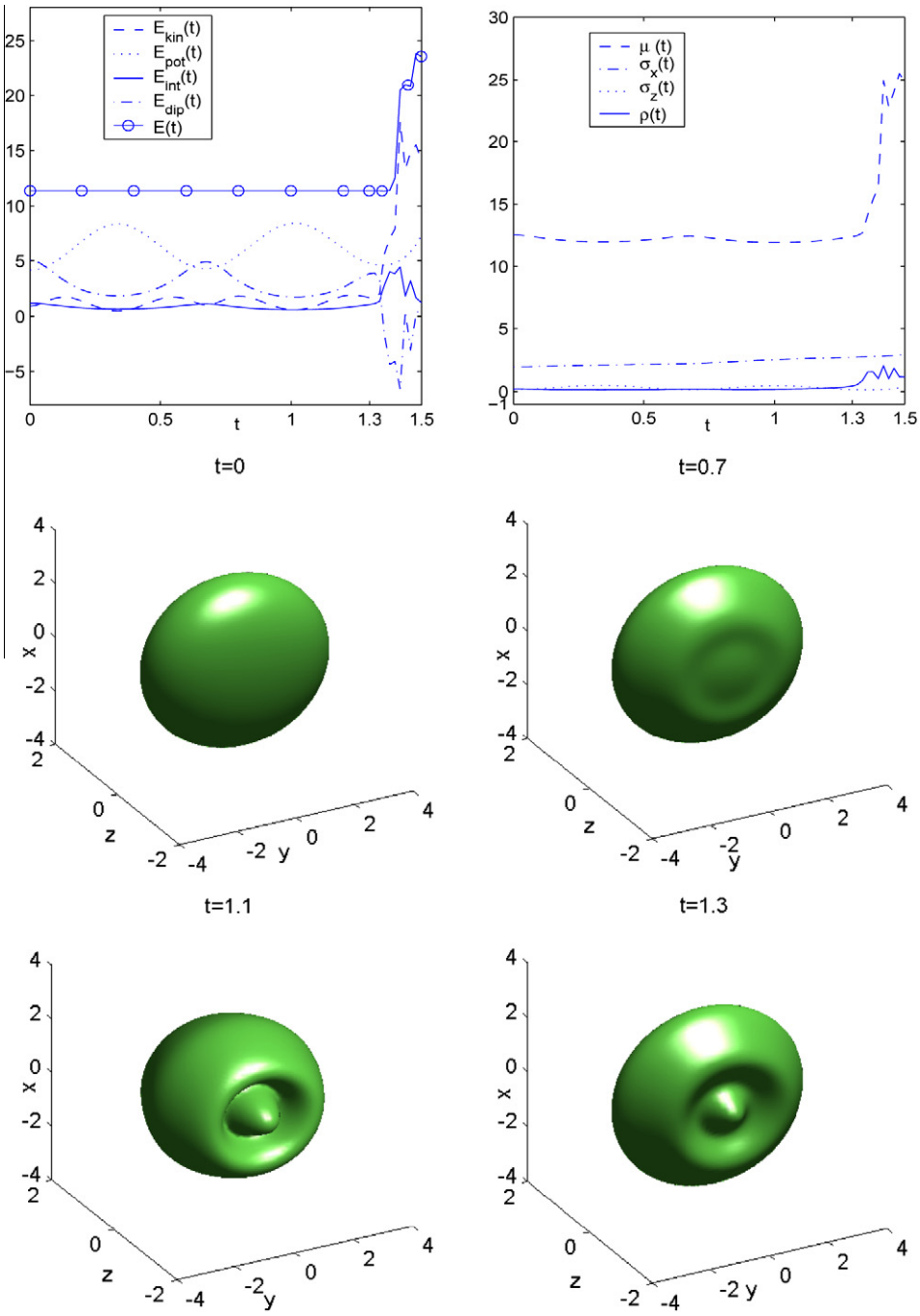

Fig. 5. Time evolution of different quantities and isosurface plots of the density function $\rho(\mathbf{x},t)$: = $|\psi(\mathbf{x},t)|^2$ = 0.01 at different times for a dipolar BEC when the dipolar interaction constant is suddenly changed from λ = 0.8 β = 82.864 to λ = 4 β = 414.32 at time t = 0.

$$\phi(\mathbf{x}, t_{n+1}) := \phi(\mathbf{x}, t_{n+1}^+) = \frac{\phi(\mathbf{x}, t_{n+1}^-)}{\|\phi(\cdot, t_{n+1}^-)\|}, \qquad \mathbf{x} \in \Omega, \quad n \geqslant 0, \tag{3.3}$$

$$\phi(\mathbf{x}, t)|_{\mathbf{x}\in\partial\Omega} = \varphi(\mathbf{x}, t)|_{\mathbf{x}\in\partial\Omega} = 0, \qquad t \geqslant 0, \tag{3.4}$$

$$\phi(\mathbf{x}, 0) = \phi_0(\mathbf{x}), \qquad \text{with} \quad \|\phi_0\| = 1; \tag{3.5}$$

where $\phi(\mathbf{x}, t_n^{\pm}) = \lim_{t\to t_n^{\pm}} \phi(\mathbf{x}, t)$.

Let M, K and L be even positive integers and define the index sets

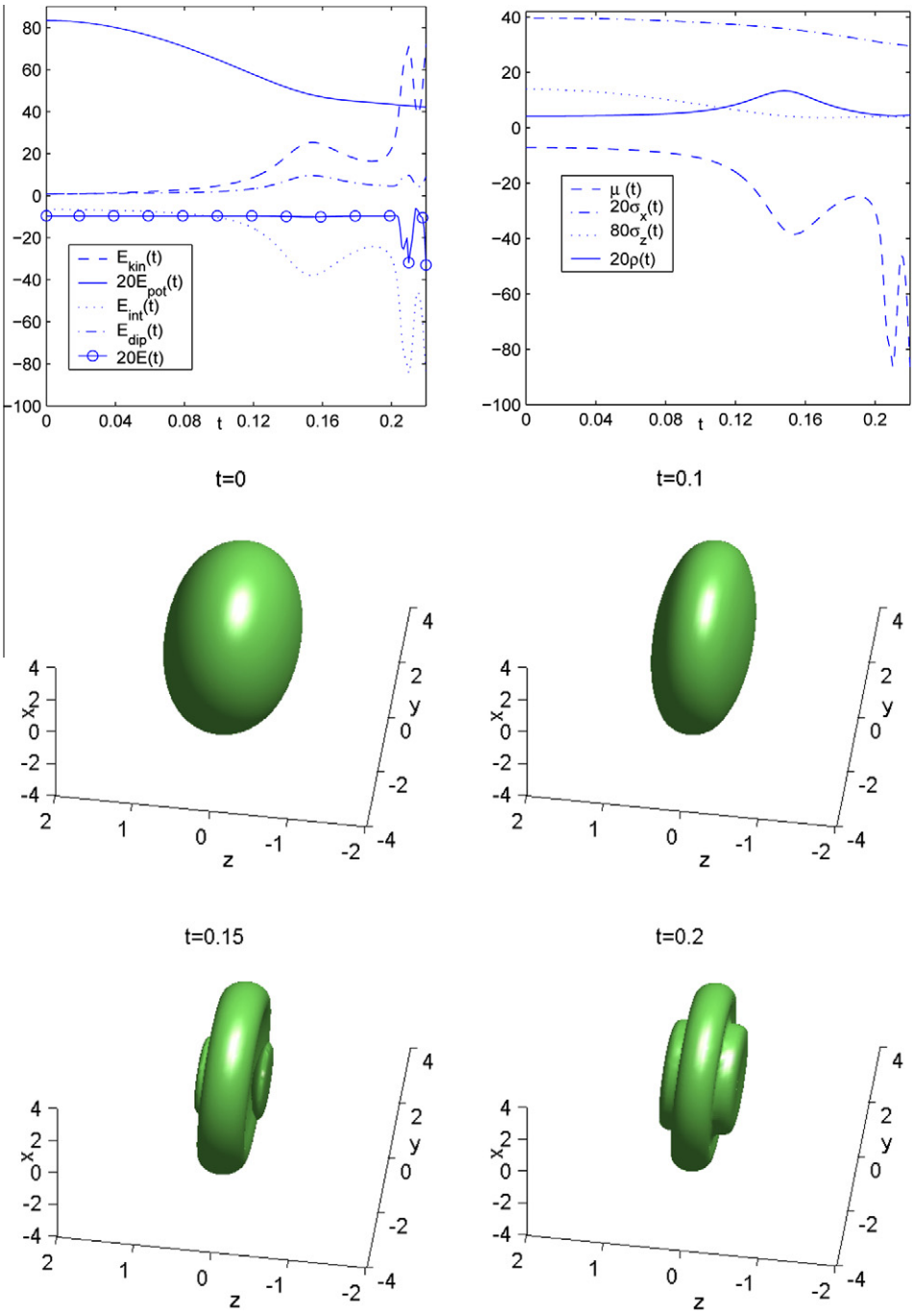

Fig. 6. Time evolution of different quantities and isosurface plots of the density function $\rho(\mathbf{x}, t)$: = $|\psi(\mathbf{x}, t)|^2$ = 0.01 at different times for a dipolar BEC when the interaction constant β is suddenly changed from β = 103.58 to β = −569.69 at time t = 0.

$$\mathcal{T}_{MKL} = \{(j,k,l)|j = 1,2,\ldots,M-1,\ k = 1,2,\ldots,K-1,\ l = 1,2,\ldots,L-1\},$$
$$\mathcal{T}^0_{MKL} = \{(j,k,l)\mid j = 0,1,\ldots,M,\ k = 0,1,\ldots,K,\ l = 0,1,\ldots,L\}.$$

Choose the spatial mesh sizes as $h_x = \frac{b-a}{M}$, $h_y = \frac{d-c}{K}$ and $h_z = \frac{f-e}{L}$ and define

$$x_j := a + j\ h_x, \qquad y_k = c + k\ h_y, \qquad z_l = e + l\ h_z, \qquad (j,k,l) \in \mathcal{T}^0_{MKL}.$$

Denote the space

$$Y_{MKL} = \mathrm{span}\{\Phi_{jkl}(\mathbf{x}), \quad (j,k,l) \in \mathcal{T}_{MKL}\},$$

with

$$\Phi_{jkl}(\mathbf{x}) = \sin\left(\mu^x_j(x-a)\right)\sin(\mu^y_k(y-c))\sin(\mu^z_l(z-e)), \quad \mathbf{x} \in \Omega, \qquad (j,k,l) \in \mathcal{T}_{MKL},$$

$$\mu^x_j = \frac{\pi j}{b-a}, \qquad \mu^y_k = \frac{\pi k}{d-c}, \qquad \mu^z_l = \frac{\pi l}{f-e}, \qquad (j,k,l) \in \mathcal{T}_{MKL};$$

and $P_{MKL}: Y = \{\varphi \in C(\Omega)\,|\,\varphi(\mathbf{x})|_{\mathbf{x}\in\partial\Omega} = 0\} \to Y_{MKL}$ be the standard project operator [38], i.e.

$$(P_{MKL}v)(\mathbf{x}) = \sum_{p=1}^{M-1}\sum_{q=1}^{K-1}\sum_{s=1}^{L-1} \widehat{v}_{pqs}\ \Phi_{pqs}(\mathbf{x}), \quad \mathbf{x} \in \Omega, \qquad \forall v \in Y,$$

with

$$\widehat{v}_{pqs} = \int_\Omega v(\mathbf{x})\ \Phi_{pqs}(\mathbf{x})\ d\mathbf{x}, \qquad (p,q,s) \in \mathcal{T}_{MKL}. \tag{3.6}$$

Then a backward Euler sine spectral discretization for (3.1)–(3.5) reads:
Find $\phi^{n+1}(\mathbf{x}) \in Y_{MKL}$ (i.e. $\phi^+(\mathbf{x}) \in Y_{MKL}$) and $\varphi^n(\mathbf{x}) \in Y_{MKL}$ such that

$$\frac{\phi^+(\mathbf{x}) - \phi^n(\mathbf{x})}{\Delta t} = \frac{1}{2}\nabla^2\phi^+(\mathbf{x}) - P_{MKL}\Big\{\Big[V(\mathbf{x}) + (\beta-\lambda)|\phi^n(\mathbf{x})|^2 + 3\lambda\tilde{\varphi}^n(\mathbf{x})\Big]\phi^+(\mathbf{x})\Big\}, \ \mathbf{x} \in \Omega, \tag{3.7}$$

$$\tilde{\varphi}^n(\mathbf{x}) = \partial_{\mathbf{nn}}\varphi^n(\mathbf{x}), \quad -\nabla^2\varphi^n(\mathbf{x}) = P_{MKL}\left(|\phi^n(\mathbf{x})|^2\right), \quad \phi^{n+1}(\mathbf{x}) = \frac{\phi^+(\mathbf{x})}{\|\phi^+(\mathbf{x})\|_2}, \quad n \geqslant 0; \tag{3.8}$$

where $\phi^0(\mathbf{x}) = P_{MKL}(\phi_0(\mathbf{x}))$ is given.

The above discretization can be solved in phase space and it is not suitable in practice due to the difficulty of computing the integrals in (3.6). We now present an efficient implementation by choosing $\phi^0(\mathbf{x})$ as the interpolation of $\phi_0(\mathbf{x})$ on the grid points $\{(x_j,y_k,z_l),\ (j,k,l) \in \mathcal{T}^0_{MKL}\}$, i.e. $\phi^0(x_j,y_k,z_l) = \phi_0(x_j,y_k,z_l)$ for $(j,k,l) \in \mathcal{T}^0_{MKL}$, and approximating the integrals in (3.6) by a quadrature rule on the grid points. Let ϕ^n_{jkl} and φ^n_{jkl} be the approximations of $\phi(x_j,y_k,z_l,t_n)$ and $\varphi(x_j,y_k,z_l,t_n)$, respectively, which are the solution of (3.1)–(3.5); denote $\rho^n_{jkl} = |\phi^n_{jkl}|^2$ and choose $\phi^0_{jkl} = \phi_0(x_j,y_k,z_l)$ for $(j,k,l) \in \mathcal{T}^0_{MKL}$. For $n = 0, 1, \ldots$, a backward Euler sine pseudospectral discretization for (3.1)–(3.5) reads:

$$\frac{\phi^+_{jkl} - \phi^n_{jkl}}{\triangle t} = \frac{1}{2}\left(\nabla^2_s\phi^+\right)\Big|_{jkl} - \left[V(x_j,y_k,z_l) + (\beta-\lambda)\left|\phi^n_{jkl}\right|^2 + 3\lambda\tilde{\varphi}^n|_{jkl}\right]\phi^+_{jkl}, \ (j,k,l) \in \mathcal{T}_{MKL}, \tag{3.9}$$

$$\tilde{\varphi}^n|_{jkl} = (\partial^s_{\mathbf{nn}}\varphi^n)|_{jkl}, \qquad -(\nabla^2_s\varphi^n)|_{jkl} = |\phi^n_{j,k,l}|^2 = \rho^n_{jkl}, \qquad \phi^{n+1}_{jkl} = \frac{\phi^+_{jkl}}{\|\phi^+\|_h}, \tag{3.10}$$

$$\phi^{n+1}_{0kl} = \phi^{n+1}_{Mkl} = \phi^{n+1}_{j0l} = \phi^{n+1}_{jKl} = \phi^{n+1}_{jk0} = \phi^{n+1}_{jkL} = 0, \qquad (j,k,l) \in \mathcal{T}^0_{MKL}, \tag{3.11}$$

$$\varphi^n_{0kl} = \varphi^n_{Mkl} = \varphi^n_{j0l} = \varphi^n_{jKl} = \varphi^n_{jk0} = \varphi^n_{jkL} = 0, \qquad (j,k,l) \in \mathcal{T}^0_{MKL}; \tag{3.12}$$

where ∇^2_s and $\partial^s_{\mathbf{nn}}$ are sine pseudospectral approximations of ∇^2 and $\partial_{\mathbf{nn}}$, respectively, defined as

$$\left(\nabla^2_s\phi^n\right)\Big|_{jkl} = -\sum_{p=1}^{M-1}\sum_{q=1}^{K-1}\sum_{s=1}^{L-1}\left[(\mu^x_p)^2 + (\mu^y_q)^2 + (\mu^z_s)^2\right](\widetilde{\phi^n})_{pqs}\sin\left(\frac{jp\pi}{M}\right)\sin\left(\frac{kq\pi}{K}\right)\sin\left(\frac{ls\pi}{L}\right),$$
$$\tilde{\varphi}^n|_{jkl} = \sum_{p=1}^{M-1}\sum_{q=1}^{K-1}\sum_{s=1}^{L-1}\frac{(\widetilde{\rho^n})_{pqs}}{(\mu^x_p)^2 + (\mu^y_q)^2 + (\mu^z_s)^2}(\partial_{\mathbf{nn}}\Phi_{pqs}(\mathbf{x}))|_{(x_j,y_k,z_l)}, \ (j,k,l) \in \mathcal{T}_{MKL}, \tag{3.13}$$

with $(\widetilde{\phi^n})_{pqs}$ $((p,q,s) \in \mathcal{T}_{MKL})$ the discrete sine transform coefficients of the vector ϕ^n as

$$(\widetilde{\phi^n})_{pqs} = \frac{8}{MKL}\sum_{j=1}^{M-1}\sum_{k=1}^{K-1}\sum_{l=1}^{L-1}\phi^n_{jkl}\sin\left(\frac{jp\pi}{M}\right)\sin\left(\frac{kq\pi}{K}\right)\sin\left(\frac{ls\pi}{L}\right), \quad (p,q,s) \in \mathcal{T}_{MKl}, \tag{3.14}$$

and the discrete h-norm is defined as

$$\|\phi^+\|_h^2 = h_x h_y h_z \sum_{j=1}^{M-1}\sum_{k=1}^{N-1}\sum_{l=1}^{L-1} |\phi_{jkl}^+|^2.$$

Similar as those in [6], the linear system (3.9)–(3.12) can be iteratively solved in phase space very efficiently via discrete sine transform and we omitted the details here for brevity.

4. A time-splitting sine pseudospectral method for dynamics

Similarly, based on the new Gross–Pitaevskii–Poisson type system (2.7) and (2.8), we will present an efficient and accurate time-splitting sine pseudospectral (TSSP) method for computing the dynamics of a dipolar BEC.

Again, in practice, the whole space problem is truncated into a bounded computational domain $\Omega = [a,b]\times[c,d]\times[e,f]$ with homogeneous Dirichlet boundary condition. From time $t = t_n$ to time $t = t_{n+1}$, the Gross–Pitaevskii–Poisson type system (2.7) and (2.8) is solved in two steps. One solves first

$$i\partial_t\psi(\mathbf{x},t) = -\frac{1}{2}\nabla^2\psi(\mathbf{x},t), \quad \mathbf{x}\in\Omega, \qquad \psi(\mathbf{x},t)|_{\mathbf{x}\in\partial\Omega} = 0, \qquad t_n \leqslant t \leqslant t_{n+1}, \tag{4.15}$$

for the time step of length Δt, followed by solving

$$i\partial_t\psi(\mathbf{x},t) = \Big[V(\mathbf{x}) + (\beta-\lambda)|\psi(\mathbf{x},t)|^2 - 3\lambda\tilde{\varphi}(\mathbf{x},t)\Big]\psi(\mathbf{x},t), \tag{4.16}$$

$$\tilde{\varphi}(\mathbf{x},t) = \partial_{\mathbf{nn}}\varphi(\mathbf{x},t), \quad \nabla^2\varphi(\mathbf{x},t) = -|\psi(\mathbf{x},t)|^2, \quad \mathbf{x}\in\Omega, \quad t_n\leqslant t\leqslant t_{n+1}; \tag{4.17}$$

$$\varphi(\mathbf{x},t)|_{\mathbf{x}\in\partial\Omega} = 0, \qquad \psi(\mathbf{x},t)|_{\mathbf{x}\in\partial\Omega} = 0, \qquad t_n\leqslant t\leqslant t_{n+1}; \tag{4.18}$$

for the same time step. Eq. (4.15) will be discretized in space by sine pseudospectral method and integrated in time *exactly* [9]. For $t\in[t_n,t_{n+1}]$, the equations (4.16)–(4.18) leave $|\psi|$ and φ invariant in t [5,9] and therefore they collapses to

$$i\partial_t\psi(\mathbf{x},t) = \Big[V(\mathbf{x}) + (\beta-\lambda)|\psi(\mathbf{x},t_n)|^2 - 3\lambda\tilde{\varphi}(\mathbf{x},t_n)\Big]\psi(\mathbf{x},t), \quad \mathbf{x}\in\Omega,\ t_n\leqslant t\leqslant t_{n+1}, \tag{4.19}$$

$$\tilde{\varphi}(\mathbf{x},t_n) = \partial_{\mathbf{nn}}\varphi(\mathbf{x},t_n), \quad -\nabla^2\varphi(\mathbf{x},t_n) = |\psi(\mathbf{x},t_n)|^2, \quad \mathbf{x}\in\Omega. \tag{4.20}$$

Again, Eq. (4.20) will be discretized in space by sine pseudospectral method [9,38] and the linear ODE (4.19) can be integrated in time *exactly* [5,9].

Let ψ_{jkl}^n and φ_{jkl}^n be the approximations of $\psi(x_j,y_k,z_l,t_n)$ and $\varphi(x_j,y_k,z_l,t_n)$, respectively, which are the solution of (2.7) and (2.8); and choose $\psi_{jkl}^0 = \psi_0(x_j,y_k,z_l)$ for $(j,k,l)\in\mathcal{T}_{MKL}^0$. For $n = 0, 1, \ldots$, a second-order TSSP method for solving (2.7) and (2.8) via the standard Strang splitting is [39,5,9]

$$\begin{aligned}
\psi_{jkl}^{(1)} &= \sum_{p=1}^{M-1}\sum_{q=1}^{K-1}\sum_{s=1}^{L-1} e^{-i\triangle t\left[(\mu_p^x)^2+(\mu_q^y)^2+(\mu_s^z)^2\right]/4}\ \widetilde{(\psi^n)}_{pqr}\sin\left(\frac{jp\pi}{M}\right)\sin\left(\frac{kq\pi}{K}\right)\sin\left(\frac{ls\pi}{L}\right),\\
\psi_{jkl}^{(2)} &= e^{-i\triangle t\left[V(x_j,y_k,z_l)+(\beta-\lambda)|\psi_{jkl}^{(1)}|^2-3\lambda\tilde{\varphi}^{(1)}|_{jkl}\right]}\ \psi_{jkl}^{(1)}, \qquad (j,k,l)\in\mathcal{T}_{MKL}^0,\\
\psi_{jkl}^{n+1} &= \sum_{p=1}^{M-1}\sum_{q=1}^{K-1}\sum_{s=1}^{L-1} e^{-i\triangle t\left[(\mu_p^x)^2+(\mu_q^y)^2+(\mu_s^z)^2\right]/4}\ \widetilde{(\psi^{(2)})}_{pqr}\sin\left(\frac{jp\pi}{M}\right)\sin\left(\frac{kq\pi}{K}\right)\sin\left(\frac{ls\pi}{L}\right);
\end{aligned} \tag{4.21}$$

where $\widetilde{(\psi^n)}_{pqs}$ and $\widetilde{(\psi^{(2)})}_{pqs}$ $((p,q,s)\in\mathcal{T}_{MKL})$ are the discrete sine transform coefficients of the vectors ψ^n and $\psi^{(2)}$, respectively (defined similar as those in (3.14)); and $\tilde{\varphi}^{(1)}|_{jkl}$ can be computed as in (3.13) with $\rho_{jkl}^n = \rho_{jkl}^{(1)} := |\psi_{jkl}^{(1)}|^2$ for $(j,k,l)\in\mathcal{T}_{MKL}^0$.

The above method is explicit, unconditionally stable, the memory cost is $O(MKL)$ and the computational cost per time step is $O(MKL\ \ln(MKL))$. In fact, for the stability, we have.

Lemma 4.1. *The TSSP method (4.21) is normalization conservation, i.e.*

$$\|\psi^n\|_h^2 := h_x h_y h_z \sum_{j=1}^{M-1}\sum_{k=1}^{K-1}\sum_{l=1}^{L-1}|\psi_{jkl}^n|^2 \equiv h_x h_y h_z \sum_{j=1}^{M-1}\sum_{k=1}^{K-1}\sum_{l=1}^{L-1}|\psi_{jkl}^0|^2 = \|\psi^0\|_h^2, \ n\geqslant 0. \tag{4.22}$$

Proof. Follow the analogous proof in [5,9] and we omit the details here for brevity. □

5. Numerical results

In this section, we first compare our new methods and the standard method used in the literatures [49,46,41,10] to evaluate numerically the dipolar energy and then report ground states and dynamics of dipolar BECs by using our new numerical methods.

5.1. Comparison for evaluating the dipolar energy

Let

$$\phi := \phi(\mathbf{x}) = \pi^{-3/4}\gamma_x^{1/2}\gamma_z^{1/4}e^{-\frac{1}{2}\left(\gamma_x(x^2+y^2)+\gamma_z z^2\right)}, \qquad \mathbf{x}\in\mathbb{R}^3. \tag{5.1}$$

Then the dipolar energy $E_{\rm dip}(\phi)$ in (2.33) can be evaluated analytically as [42]

$$E_{\rm dip}(\phi) = -\frac{\lambda\gamma_x\sqrt{\gamma_z}}{4\pi\sqrt{2\pi}}\begin{cases} \frac{1+2\kappa^2}{1-\kappa^2} - \frac{3\kappa^2\arctan\left(\sqrt{\kappa^2-1}\right)}{(1-\kappa^2)\sqrt{\kappa^2-1}}, & \kappa>1,\\ 0, & \kappa=1,\\ \frac{1+2\kappa^2}{1-\kappa^2} - \frac{1.5\kappa^2}{(1-\kappa^2)\sqrt{1-\kappa^2}}\ln\left(\frac{1+\sqrt{1-\kappa^2}}{1-\sqrt{1-\kappa^2}}\right), & \kappa<1, \end{cases} \tag{5.2}$$

with $\kappa = \sqrt{\frac{\gamma_z}{\gamma_x}}$. This provides a perfect example to test the efficiency of different numerical methods to deal with the dipolar potential. Based on our new formulation (2.33), the dipolar energy can be evaluated via discrete sine transform (DST) as

$$E_{\rm dip}(\phi) \approx \frac{\lambda h_x h_y h_z}{2}\sum_{j=1}^{M-1}\sum_{k=1}^{K-1}\sum_{l=1}^{L-1}|\phi(x_j,y_k,z_l)|^2\left[-|\phi(x_j,y_k,z_l)|^2 - 3\tilde{\varphi}|_{jkl}\right],$$

where $\tilde{\varphi}|_{jkl}$ is computed as in (3.13) with $\rho^n_{jkl} = |\phi(x_j,y_k,z_l)|^2$ for $(j,k,l)\in\mathcal{T}^0_{MKL}$. In the literatures [49,41,46,10], this dipolar energy is usually calculated via discrete Fourier transform (DFT) as

$$E_{\rm dip}(\phi) \approx \frac{\lambda h_x h_y h_z}{2}\sum_{j=0}^{M-1}\sum_{k=0}^{K-1}\sum_{l=0}^{L-1}|\phi(x_j,y_k,z_l)|^2\left[\mathcal{F}^{-1}_{jkl}\left(\widehat{(U_{\rm dip})}(2\mu^x_p,2\mu^y_q,2\mu^z_s)\cdot\mathcal{F}_{pqs}(|\phi|^2)\right)\right],$$

where $\mathcal{F}$ and $\mathcal{F}^{-1}$ are the discrete Fourier and inverse Fourier transforms over the grid points $\{(x_j,y_k,z_l),(j,k,l)\in\mathcal{T}^0_{MKL}\}$, respectively [46]. We take $\lambda = 24\pi$, the bounded computational domain $\Omega = [-16,16]^3$, $M = K = L$ and thus $h = h_x = h_y = h_z = \frac{32}{M}$. Table 1 lists the errors $e := |E_{\rm dip}(\phi) - E^h_{\rm dip}|$ with $E^h_{\rm dip}$ computed numerically via either (5.3) or (5.3) with mesh size h for three cases:

- Case I. $\gamma_x = 0.25$ and $\gamma_z = 1$ which implies $\kappa = 2.0$ and $E_{\rm dip}(\phi) = 0.0386708614$;
- Case II. $\gamma_x = \gamma_z = 1$ which implies $\kappa = 1.0$ and $E_{\rm dip}(\phi) = 0$;
- Case III. $\gamma_x = 2$ and $\gamma_z = 1$ which implies $\kappa = \sqrt{0.5}$ and $E_{\rm dip}(\phi) = -0.1386449741$.

From Table 1 and our extensive numerical results not shown here for brevity, we can conclude that our new method via discrete sine transform based on a new formulation is much more accurate than that of the standard method via discrete Fourier transform in the literatures for evaluating the dipolar energy.

5.2. Ground states of dipolar BECs

By using our new numerical method (3.9)–(3.12), here we report the ground states of a dipolar BEC (e.g., ^{52}Cr [30]) with different parameters and trapping potentials. In our computation and results, we always use the dimensionless quantities. We take $M = K = L = 128$, time step $\Delta t = 0.01$, dipolar direction $\mathbf{n} = (0,0,1)^T$ and the bounded computational domain $\Omega = [-8,8]^3$ for all cases except $\Omega = [-16,16]^3$ for the cases $\frac{N}{10000} = 1,\ 5,\ 10$ and $\Omega = [-20,20]^3$ for the cases $\frac{N}{10000} = 50,\ 100$ in Table 2. The ground state ϕ_g is reached numerically when $\|\phi^{n+1}-\phi^n\|_\infty := \max_{0\leqslant j\leqslant M,\ 0\leqslant k\leqslant K,\ 0\leqslant l\leqslant L}|\phi^{n+1}_{jkl}-\phi^n_{jkl}| \leqslant \varepsilon := 10^{-6}$ in (3.9)–(3.12). Table 2 shows the energy $E^g := E(\phi_g)$, chemical potential $\mu^g := \mu(\phi_g)$, kinetic energy $E^g_{\rm kin} := E_{\rm kin}(\phi_g)$, potential energy $E^g_{\rm pot} := E_{\rm pot}(\phi_g)$, interaction energy $E^g_{\rm int} := E_{\rm int}(\phi_g)$, dipolar energy $E^g_{\rm dip} := E_{\rm dip}(\phi_g)$, condensate widths $\sigma^g_x := \sigma_x(\phi_g)$ and $\sigma^g_z := \sigma_z(\phi_g)$ in (2.38) and central density $\rho_g(\mathbf{0}) := |\phi_g(0,0,0)|^2$ with harmonic potential $V(x,y,z) = \frac{1}{2}(x^2+y^2+0.25z^2)$ for different $\beta = 0.20716N$ and $\lambda = 0.033146N$ with N the total number of particles in the condensate; and Table 3 lists similar results with $\beta = 207.16$ for different values of $-0.5\leqslant\frac{\lambda}{\beta}\leqslant 1$. In addition, Fig. 1 depicts the ground state $\phi_g(\mathbf{x})$, e.g. surface plots of $|\phi_g(x,0,z)|^2$ and isosurface plots of $|\phi_g(\mathbf{x})| = 0.01$, of a dipolar BEC with $\beta = 401.432$ and $\lambda = 0.16\beta$ for harmonic potential $V(\mathbf{x}) = \frac{1}{2}(x^2+y^2+z^2)$, double-well potential $V(\mathbf{x}) = \frac{1}{2}(x^2+y^2+z^2) + 4e^{-z^2/2}$ and optical lattice potential $V(\mathbf{x}) = \frac{1}{2}(x^2+y^2+z^2) + 100[\sin^2(\frac{\pi}{2}x)+\sin^2(\frac{\pi}{2}y)+\sin^2(\frac{\pi}{2}z)]$; and Fig. 2 depicts the ground state $\phi_g(\mathbf{x})$, e.g. isosurface plots of $|\phi_g(\mathbf{x})| = 0.08$, of a dipolar BEC with the harmonic potential $V(\mathbf{x}) = \frac{1}{2}(x^2+y^2+z^2)$ and $\beta = 207.16$ for different values of $-0.5\leqslant\frac{\lambda}{\beta}\leqslant 1$.

From Tables 2 and 3 and Figs. 1 and 2, we can draw the following conclusions: (i) For fixed trapping potential $V(\mathbf{x})$ and dipolar direction $\mathbf{n} = (0,0,1)^T$, when β and λ increase with the ratio $\frac{\lambda}{\beta}$ fixed, the energy E^g, chemical potential μ^g, potential energy $E^g_{\rm pot}$, interaction energy $E^g_{\rm int}$, condensate widths σ^g_x and σ^g_z of the ground states increase; and resp., the kinetic energy $E^g_{\rm kin}$, dipolar energy $E^g_{\rm dip}$ and central density $\rho_g(\mathbf{0})$ decrease (cf. Table 2). (ii) For fixed trapping potential $V(\mathbf{x})$, dipolar direction

$\mathbf{n} = (0,0,1)^T$ and β, when the ratio $\frac{\lambda}{\beta}$ increases from -0.5 to 1, the kinetic energy $E^g_{\rm kin}$, interaction energy $E^g_{\rm int}$, condensate widths σ^g_z and central density $\rho_g(\mathbf{0})$ of the ground states increase; and resp., the energy E^g, chemical potential μ^g, potential energy $E^g_{\rm pot}$, dipolar energy $E^g_{\rm dip}$ and condensate widths σ^g_x decrease (cf. Table 3). (iii) Our new numerical method can compute the ground states accurately and efficiently (cf. Figs. 1 and 2).

5.3. Dynamics of dipolar BECs

Similarly, by using our new numerical method (4.21), here we report the dynamics of a dipolar BEC (e.g., ^{52}Cr [30]) under different setups. Again, in our computation and results, we always use the dimensionless quantities. We take the bounded computational domain $\Omega = [-8,8]^2 \times [-4,4]$, $M = K = L = 128$, i.e. $h = h_x = h_y = 1/8, h_z = 1/16$, time step $\Delta t = 0.001$. The initial data $\psi(\mathbf{x},0) = \psi_0(\mathbf{x})$ is chosen as the ground state of a dipolar BEC computed numerically by our numerical method with $\mathbf{n} = (0,0,1)^T$, $V(\mathbf{x}) = \frac{1}{2}(x^2 + y^2 + 25z^2)$, $\beta = 103.58$ and $\lambda = 0.8\beta = 82.864$.

The first case to study numerically is the dynamics of suddenly changing the dipolar direction from $\mathbf{n} = (0,0,1)^T$ to $\mathbf{n} = (1,0,0)^T$ at $t = 0$ and keeping all other quantities unchanged. Fig. 3 depicts time evolution of the energy $E(t) := E(\psi(\cdot,t))$, chemical potential $\mu(t) = \mu(\psi(\cdot,t))$, kinetic energy $E_{\rm kin}(t) := E_{\rm kin}(\psi(\cdot,t))$, potential energy $E_{\rm pot}(t) := E_{\rm pot}(\psi(\cdot,t))$, interaction energy $E_{\rm int}(t) := E_{\rm int}(\psi(\cdot,t))$, dipolar energy $E_{\rm dip}(t) := E_{\rm dip}(\psi(\cdot,t))$, condensate widths $\sigma_x(t) := \sigma_x(\psi(\cdot,t))$, $\sigma_z(t) := \sigma_z(\psi(\cdot,t))$, and central density $\rho(t) := |\psi(\mathbf{0},t)|^2$, as well as the isosurface of the density function $\rho(\mathbf{x},t) := |\psi(\mathbf{x},t)|^2 = 0.01$ for different times. In addition, Fig. 4 show similar results for the case of suddenly changing the trapping potential from $V(\mathbf{x}) = \frac{1}{2}(x^2 + y^2 + 25z^2)$ to $V(\mathbf{x}) = \frac{1}{2}(x^2 + y^2 + \frac{25}{4}z^2)$ at $t = 0$, i.e. decreasing the trapping frequency in z-direction from 5 to $\frac{5}{2}$, and keeping all other quantities unchanged; Fig. 5 show the results for the case of suddenly changing the dipolar interaction from $\lambda = 0.8$ $\beta = 82.864$ to $\lambda = 4$ $\beta = 414.32$ at $t = 0$ while keeping all other quantities unchanged, i.e. collapse of a dipolar BEC; and Fig. 6 show the results for the case of suddenly changing the interaction constant β from $\beta = 103.58$ to $\beta = -569.69$ at $t = 0$ while keeping all other quantities unchanged, i.e. another collapse of a dipolar BEC.

From Figs. 3–6, we can conclude that the dynamics of dipolar BEC can be very interesting and complicated. In fact, global existence of the solution is observed in the first two cases (cf. Figs. 3 and 4) and finite time blow-up is observed in the last two cases (cf. Figs. 5 and 6). The total energy is numerically conserved very well in our computation when there is no blow-up (cf. Figs. 3 and 4) and before blow-up happens (cf. Figs. 5 and 6). Of course, it is not conserved numerically near or after blow-up happens because the mesh size and time step are fixed which cannot resolve the solution. In addition, our new numerical method can compute the dynamics of dipolar BEC accurately and efficiently.

6. Conclusions

Efficient and accurate numerical methods were proposed for computing ground states and dynamics of dipolar Bose–Einstein condensates based on the three-dimensional Gross–Pitaevskii equation (GPE) with a nonlocal dipolar interaction potential. By decoupling the dipolar interaction potential into a short-range and a long-range part, the GPE for a dipolar BEC is re-formulated to a Gross–Pitaevskii–Poisson type system. Based on this new mathematical formulation, we proved rigorously the existence and uniqueness as well as nonexistence of the ground states, and discussed the dynamical properties of dipolar BEC in different parameter regimes. In addition, the backward Euler sine pseudospectral method and time-splitting sine pseudospectral method were proposed for computing the ground states and dynamics of a dipolar BEC, respectively. Our new numerical methods avoided taking the Fourier transform of the nonlocal dipolar interaction potential which is highly singular and causes some numerical difficulties in practical computation. Comparison between our new numerical methods and existing numerical methods in the literatures showed that our numerical methods perform better. Applications of our new numerical methods for computing the ground states and dynamics of dipolar BECs were reported. In the future, we will use our new numerical methods to simulate the ground states and dynamics of dipolar BEC with experimental relevant setups and extend our methods for rotating dipolar BECs.

Acknowledgements

This work was supported in part by the Academic Research Fund of Ministry of Education of Singaporegrant R-146-000-120-112 (W.B., Y.C. and H.W.) and the National Natural Science Foundation of China grant 10901134 (H.W.). The authors would like to acknowledge very stimulating and helpful discussions with Professor Peter A. Markowich on the topic. This work was partially done while the authors were visiting the Institute for Mathematical Sciences, National University of Singapore, in 2009.

Appendix A. Proof of the equality (2.2)

Let

$$\phi(\mathbf{x}) = \frac{3}{4\pi r^3}\left(1 - \frac{3(\mathbf{x}\cdot\mathbf{n})^2}{r^2}\right), \qquad r = |\,\mathbf{x}\,|, \qquad \mathbf{x} \in \mathbb{R}^3. \tag{A.1}$$

For any $\mathbf{n} \in \mathbb{R}^3$ satisfies $|\mathbf{n}| = 1$, in order to prove (2.2) holds in the distribution sense, it is equivalent to prove the following:

$$\int_{\mathbb{R}^3} \phi(\mathbf{x}) f(\mathbf{x}) d\mathbf{x} = -f(\mathbf{0}) - 3 \int_{\mathbb{R}^3} f(\mathbf{x})\ \partial_{\mathbf{nn}} \left(\frac{1}{4\pi r}\right) d\mathbf{x}, \qquad \forall f(\mathbf{x}) \in C_0^\infty(\mathbb{R}^3). \tag{A.2}$$

For any fixed $\varepsilon > 0$, let $B_\varepsilon = \{\mathbf{x} \in \mathbb{R}^3 \mid |\mathbf{x}| < \varepsilon\}$ and $B_\varepsilon^c = \{\mathbf{x} \in \mathbb{R}^3 \mid |\mathbf{x}| \geqslant \varepsilon\}$. It is straightforward to check that

$$\phi(\mathbf{x}) = -3\partial_{\mathbf{nn}} \left(\frac{1}{4\pi r}\right), \qquad 0 \neq \mathbf{x} \in \mathbb{R}^3. \tag{A.3}$$

Using integration by parts and noticing (A.3), we get

$$\begin{aligned} \int_{B_\varepsilon^c} \phi(\mathbf{x}) f(\mathbf{x}) d\mathbf{x} &= -3 \int_{B_\varepsilon^c} f(\mathbf{x})\ \partial_{\mathbf{nn}} \left(\frac{1}{4\pi r}\right) d\mathbf{x} = 3 \int_{B_\varepsilon^c} \partial_{\mathbf{n}} \left(\frac{1}{4\pi r}\right)\ \partial_{\mathbf{n}}(f(\mathbf{x}))\ d\mathbf{x} + 3 \int_{\partial B_\varepsilon} f(\mathbf{x})\ \frac{\mathbf{n}\cdot\mathbf{x}}{r}\ \partial_{\mathbf{n}} \left(\frac{1}{4\pi r}\right) dS \\ &= -3 \int_{B_\varepsilon^c} \frac{1}{4\pi r}\ \partial_{\mathbf{nn}}(f(\mathbf{x}))\ d\mathbf{x} + I_1^\varepsilon + I_2^\varepsilon, \end{aligned} \tag{A.4}$$

where

$$I_1^\varepsilon := 3 \int_{\partial B_\varepsilon} f(\mathbf{x})\ \frac{\mathbf{n}\cdot\mathbf{x}}{r}\ \partial_{\mathbf{n}} \left(\frac{1}{4\pi r}\right) dS, \qquad I_2^\varepsilon := -3 \int_{\partial B_\varepsilon} \frac{\mathbf{n}\cdot\mathbf{x}}{4\pi r^2}\ \partial_{\mathbf{n}}(f(\mathbf{x}))\, dS. \tag{A.5}$$

From (A.5), changing of variables, we get

$$\begin{aligned} I_1^\varepsilon &= -3 \int_{\partial B_\varepsilon} \frac{(\mathbf{n}\cdot\mathbf{x})^2}{4\pi r^4} f(\mathbf{x})\, dS = -\frac{3}{4\pi} \int_{\partial B_1} \frac{(\mathbf{n}\cdot\mathbf{x})^2}{\varepsilon^2} f(\varepsilon\mathbf{x})\, \varepsilon^2 dS \\ &= -\frac{3}{4\pi} \int_{\partial B_1} (\mathbf{n}\cdot\mathbf{x})^2 f(\mathbf{0})\, dS - \frac{3}{4\pi} \int_{\partial B_1} (\mathbf{n}\cdot\mathbf{x})^2 [f(\varepsilon\mathbf{x}) - f(\mathbf{0})]\, dS. \end{aligned} \tag{A.6}$$

Choosing $0 \neq \mathbf{n}_1 \in \mathbb{R}^3$ and $0 \neq \mathbf{n}_2 \in \mathbb{R}^3$ such that $\{\mathbf{n}_1, \mathbf{n}_2, \mathbf{n}\}$ forms an orthornormal basis of $\mathbb{R}^3$, by symmetry, we obtain

$$A := \frac{3}{4\pi} \int_{\partial B_1} (\mathbf{n}\cdot\mathbf{x})^2\, dS = \frac{1}{4\pi} \int_{\partial B_1} \left[(\mathbf{n}\cdot\mathbf{x})^2 + (\mathbf{n}_1\cdot\mathbf{x})^2 + (\mathbf{n}_2\cdot\mathbf{x})^2\right] dS = \frac{1}{4\pi} \int_{\partial B_1} |\mathbf{x}|^2 dS = \frac{1}{4\pi} \int_{\partial B_1} dS = 1, \tag{A.7}$$

$$\left| \int_{\partial B_1} (\mathbf{n}\cdot\mathbf{x})^2 (f(\varepsilon\mathbf{x}) - f(\mathbf{0}))\, dS \right| = \left| \int_{\partial B_1} (\mathbf{n}\cdot\mathbf{x})^2 \varepsilon\ [\mathbf{x}\cdot\nabla f(\theta\varepsilon\mathbf{x})]\, dS \right| \leqslant \varepsilon \|\nabla f\|_{L^\infty(B_\varepsilon)} \int_{\partial B_1} dS \leqslant 4\pi\varepsilon \|\nabla f\|_{L^\infty(B_\varepsilon)}, \tag{A.8}$$

where $0 \leqslant \theta \leqslant 1$. Plugging (A.7) and (A.8) into (A.6), we have

$$I_1^\varepsilon \to -f(\mathbf{0}), \qquad \varepsilon \to 0^+. \tag{A.9}$$

Similarly, for $\varepsilon \to 0^+$, we get

$$|I_2^\varepsilon| \leqslant 3\|\nabla f\|_{L^\infty(B_\varepsilon)} \int_{\partial B_\varepsilon} \frac{1}{4\pi\varepsilon}\, dS = 3\varepsilon \|\nabla f\|_{L^\infty(B_\varepsilon)} \to 0, \tag{A.10}$$

$$\left| \int_{B_\varepsilon} \frac{3}{4\pi r}\ \partial_{\mathbf{nn}}(f(\mathbf{x}))\, d\mathbf{x} \right| \leqslant \|D^2 f\|_{L^\infty(B_\varepsilon)} \int_{B_\varepsilon} \frac{3}{4\pi}\, d\mathbf{x} \leqslant \frac{3}{2}\varepsilon^2 \|D^2 f\|_{L^\infty(B_\varepsilon)} \to 0. \tag{A.11}$$

Combining (A.9), (A.10) and (A.11), taking $\varepsilon \to 0^+$ in (A.4), we obtain

$$\int_{\mathbb{R}^3} \phi(\mathbf{x}) f(\mathbf{x}) d\mathbf{x} = -f(\mathbf{0}) - 3 \int_{\mathbb{R}^3} \frac{1}{4\pi r}\ \partial_{\mathbf{nn}}(f(\mathbf{x}))\, d\mathbf{x}, \qquad \forall f(\mathbf{x}) \in C_0^\infty(\mathbb{R}^3). \tag{A.12}$$

Thus (A.2) follows from (A.12) and the definition of the derivative in the distribution sense, i.e.

$$\int_{\mathbb{R}^3} f(\mathbf{x})\ \partial_{\mathbf{nn}} \left(\frac{1}{4\pi r}\right) d\mathbf{x} = \int_{\mathbb{R}^3} \frac{1}{4\pi r}\ \partial_{\mathbf{nn}}(f(\mathbf{x}))\, d\mathbf{x}, \qquad \forall f(\mathbf{x}) \in C_0^\infty(\mathbb{R}^3), \tag{A.13}$$

and the equality (2.2) is proven. □

References

[1] M. Abad, M. Guilleumas, R. Mayol, M. Pi, Vortices in Bose–Einstein condensates with dominant dipolar interactions, Phys. Rev. A 79 (2009) (Article 063622).
[2] P. Antonelli, C. Sparber, Existence of solitary waves in dipolar quantum gases, preprint.
[3] W. Bao, Ground states and dynamics of multi-component Bose–Einstein condensates, Multiscale Model. Simul. 2 (2004) 210–236.
[4] W. Bao, Q. Du, Computing the ground state solution of Bose–Einstein condensates by a normalized gradient flow, SIAM J. Sci. Comput. 25 (2004) 1674–1697.
[5] W. Bao, D. Jaksch, P.A. Markowich, Numerical solution of the Gross–Pitaevskii equation for Bose–Einstein condensation, J. Comput. Phys. 187 (2003) 318–342.
[6] W. Bao, I.-L. Chern, F.Y. Lim, Efficient and spectrally accurate numerical methods for computing ground and first excited states in Bose–Einstein condensates, J. Comput. Phys. 219 (2006) 836–854.

[7] W. Bao, W. Tang, Ground state solution of Bose–Einstein condensate by directly minimizing the energy functional, J. Comput. Phys. 187 (2003) 230–254.
[8] W. Bao, H. Wang, P.A. Markowich, Ground state, symmetric and central vortex state in rotating Bose–Einstein condensate, Commun. Math. Sci. 3 (2005) 57–88.
[9] W. Bao, Y. Zhang, Dynamics of the ground state and central vortex states in Bose-Einstein condensation, Math. Models Methods Appl. Sci. 15 (2005) 1863–1896.
[10] P.B. Blakie, C. Ticknor, A.S. Bradley, A.M. Martin, M.J. Davis, Y. Kawaguchi, Numerical method for evolving the dipolar projected Gross–Pitaevskii equation, Phys. Rev. E 80 (2009) (Aritcle 016703).
[11] M. Caliari, A. Ostermann, S. Rainer, M. Thalhammer, A minimisation approach for computing the ground state of Gross–Pitaevskii systems, J. Comput. Phys. 228 (2009) 349–360.
[12] R. Carles, P. A Markowich, C. Sparber, On the Gross–Pitaevskii equation for trapped dipolar quantum gases, Nonlinearity 21 (2008) 2569–2590.
[13] T. Cazenave, Semilinear Schrödinger equations, Courant Lecture Notes in Mathematics, vol. 10, New York University Courant Institute of Mathematical Sciences AMS, 2003.
[14] S.M. Chang, W.W. Lin, S.F. Shieh, Gauss-Seidel-type methods for energy states of a multi-component Bose–Einstein condensate, J. Comput. Phys. 202 (2005) 367–390.
[15] M.L. Chiofalo, S. Succi, M.P. Tosi, Ground state of trapped interacting Bose–Einstein condensates by an explicit imaginary-time algorithm, Phys. Rev. E 62 (2000) 7438–7444.
[16] C. Eberlein, S. Giovanazzi, D.H.J. O'Dell, Exact solution of the Thomas-Fermi equation for a trapped Bose–Einstein condensate with dipole–dipole interactions, Phys. Rev. A 71 (2005) (Article 033618).
[17] M.S. Ellio, J.J. Valentini, D.W. Chandler, Subkelvin cooling NO molecules via "billiard-like" collisions with argon, Science 302 (2003) 1940–1943.
[18] S. Giovanazzi, P. Pedri, L. Santos, A. Griesmaier, M. Fattori, T. Koch, J. Stuhler, T. Pfau, Expansion dynamics of a dipolar Bose–Einstein condensate, Phys. Rev. A 74 (2006) (Article 013621).
[19] K. Glaum, A. Pelster, Bose–Einstein condensation temperature of dipolar gas in anisotropic harmonic trap, Phys. Rev. A 76 (2007) (Article 023604).
[20] K. Go'ral, K. Rzayewski, T. Pfau, Bose–Einstein condensation with magnetic dipole–dipole forces, Phys. Rev. A 61 (2000) 051601(R).
[21] K. Go'ral, L. Santos, Ground state and elementary excitations of single and binary Bose–Einstein condensates of trapped dipolar gases, Phys. Rev. A 66 (2002) (Article 023613).
[22] A. Griesmaier, J. Werner, S. Hensler, J. Stuhler, T. Pfau, Bose–Einstein condensation of Chromium, Phys. Rev. Lett. 94 (2005) (Article 160401).
[23] T.F. Jiang, W.C. Su, Ground state of the dipolar Bose–Einstein condensate, Phys. Rev. A 74 (2006) (Article 063602).
[24] M. Klawunn, R. Nath, P. Pedri, L. Santos, Transverse instability of straight vortex lines in dipolar Bose–Einstein condensates, Phys. Rev. Lett. 100 (2008) (Article 240403).
[25] T. Lahaye, J. Metz, B. Fröhlich, T. Koch, M. Meister, A. Griesmaier, T. Pfau, H. Saito, Y. Kawaguchi, M. Ueda, D-wave collapse and explosion of a dipolar Bose–Einstein condensate, Phys. Rev. Lett. 101 (2008) (Article 080401).
[26] E.H. Lieb, R. Seiringer, J. Yngvason, Bosons in a trap: a rigorous derivation of the Gross–Pitaevskii energy functional, Phys. Rev. A 61 (2000) (Article 043602).
[27] R. Nath, P. Pedri, L. Santos, Soliton-soliton scattering in dipolar Bose–Einstein condensates, Phys. Rev. A 76 (2007) (Article 013606).
[28] D.H.J. O'Dell, S. Giovanazzi, C. Eberlein, Exact hydrodynamics of a trapped dipolar Bose–Einstein condensate, Phys. Rev. Lett. 92 (2004) (Article 250401).
[29] D.H.J. O'Dell, C. Eberlein, Vortex in a trapped Bose–Einstein condensate with dipole–dipole interactions, Phys. Rev. A 75 (2007) (Article 013604).
[30] N.G. Parker, C. Ticknor, A.M. Martin, D.H.J. O'Dell1, Structure formation during the collapse of a dipolar atomic Bose–Einstein condensate, Phys. Rev. A 79 (2009) (Article 013617).
[31] L.P. Pitaevskii, S. Stringari, Bose–Einstein Condensation, Oxford University, New York, 2003.
[32] P. Pedri, L. Santos, Two-dimensional bright solitons in dipolar Bose–Einstein condensates, Phys. Rev. Lett. 95 (2005) (Article 200404).
[33] A. Recati, I. Carusotto, C. Lobo, S. Stringari, Dipole polarizability of a trapped superfluid Fermi gas, Phys. Rev. Lett. 97 (2006) (Article 190403).
[34] S. Ronen, D.C.E. Bortolotti, J.L. Bohn, Bogoliubov modes of a dipolar condensate in a cylindrical trap, Phys. Rev. A 74 (2006) (Article 013623).
[35] J.M. Sage, S. Sainis, T. Bergeman, D. DeMille, Optical production of ultracold polar molecules, Phys. Rev. Lett. 94 (2005) (Article 203001).
[36] L. Santos, G. Shlyapnikov, P. Zoller, M. Lewenstein, Bose–Einstein condesation in trapped dipolar gases, Phys. Rev. Lett. 85 (2000) 1791–1797.
[37] B.I. Schneider, D.L. Feder, Numerical approach to the ground and excited states of a Bose–Einstein condensed gas confined in a completely anisotropic trap, Phys. Rev. A 59 (1999) 2232–2242.
[38] J. Shen, T. Tang, Spectral and High-Order Methods with Applications, Science Press, Beijing, 2006.
[39] G. Strang, On the construction and comparison of difference schemes, SIAM J. Numer. Anal. 5 (1968) 505–517.
[40] C. Sulem, P.-L. Sulem, The Nonlinear Schrödinger Equation, Self-focusing and Wave Collapse, Springer-Verlag, New York, 1999.
[41] C. Ticknor, N.G. Parker, A. Melatos, S.L. Cornish, D.H.J. O'Dell, A.M. Martin, Collapse times of dipolar Bose–Einstein condensates, Phys. Rev. A 78 (2008) (Article 061607).
[42] I. Tikhonenkov, B.A. Malomed, A. Vardi, Anisotropic solitons in dipolar Bose–Einstein condensates, Phys. Rev. Lett. 100 (2008) (Article 090406).
[43] D. Wang, J. Qi, M.F. Stone, O. Nikolayeva, H. Wang, B. Hattaway, S.D. Gensemer, P.L. Gould, E.E. Eyler, W.C. Stwalley, Photoassociative production and trapping of ultracold K-Rb molecules, Phys. Rev. Lett. 93 (2004) (Article 243005).
[44] R.M. Wilson, S. Ronen, J.L. Bohn, Stability and excitations of a dipolar Bose–Einstein condensate with a vortex, Phys. Rev. A 79 (2009) (Article 013621).
[45] R.M. Wilson, S. Ronen, J.L. Bohn, H. Pu, Manifestations of the roton mode in dipolar Bose–Einstein condensates, Phys. Rev. Lett. 100 (2008) (Article 245302).
[46] B. Xiong, J. Gong, H. Pu, W. Bao, B. Li, Symmetry breaking and self-trapping of a dipolar Bose–Einstein condensate in a double-well potential, Phys. Rev. A 79 (2009) (Article 013626).
[47] S. Yi, H. Pu, Vortex structures in dipolar condensates, Phys. Rev. A 73 (2006) (Article 061602(R)).
[48] S. Yi, L. You, Trapped atomic condensates with anisotropic interactions, Phys. Rev. A 61 (2000) (Article 041604(R)).
[49] S. Yi, L. You, Trapped condensates of atoms with dipole interactions, Phys. Rev. A 63 (2001) (Article 053607).
[50] S. Yi, L. You, Expansion of a dipolar condensate, Phys. Rev. A 67 (2003) (Article 045601).
[51] S. Yi, L. You, Calibrating dipolar interaction in an atomic condensate, Phys. Rev. Lett. 92 (2004) (Article 193201).
[52] J. Zhang, H. Zhai, Vortex lattice in planar Bose–Einstein condensates with dipolar interactions, preprint.